HYDROCRACKING OF HEAVY OIL USING NI, FE AND MO BASED DISPERSED CATALYSTS

BY

AHMAD HASSAN ALI AL-RASHIDY

A Thesis Presented to the
DEANSHIP OF GRADUATE STUDIES

KING FAHD UNIVERSITY OF PETROLEUM & MINERALS

DHAHRAN, SAUDI ARABIA

In Partial Fulfillment of the
Requirements for the Degree of

MASTER OF SCIENCE

In

CHEMICAL ENGINEERING

DECEMBER 2015

KING FAHD UNIVERSITY OF PETROLEUM & MINERALS

DHAHRAN- 31261, SAUDI ARABIA

DEANSHIP OF GRADUATE STUDIES

This thesis, written by **Ahmad Hassan Ali Al-Rashidy** under the direction his thesis advisor and approved by his thesis committee, has been presented and accepted by the Dean of Graduate Studies, in partial fulfillment of the requirements for the degree of **MASTER OF SCIENCE IN CHEMICAL ENGINEERING.**

Shaikh Abdur Razzak

Dr. Shaikh Abdur Razzak
(Advisor)

Dr. Mohammed S. Ba-Shammakh
Department Chairman

Mozahar Hossain

Dr. Mohammad Mozahar Hossain
(Co-Advisor)

Dr. Salam A. Zummo
Dean of Graduate Studies

Dr. Sulaiman S. Al-Khattaf
(Member)

30/12/15

Date: 12/27/2015

Dr. Mohammed S. Ba-Shammakh
(Member)

Dr. Saad A. Bogami
(Member)

Dedication

This work is dedicated to my late father Hassan Ali Al-Rashidy and my mother Sanaa Al-Dakaa for their constant support, love and their patience with me.

ACKNOWLEDGMENTS

All Praises and gratitude to almighty Allah for giving me strength, endurance and patience to complete this work successfully. I thank him for guiding me to this point of my career and the uncountable favors he has bestowed on me. Thereafter, I am thankful to King Fahd University of Petroleum and Minerals for giving me the chance to pursue my graduate studies. I would like to express my deepest gratitude to my thesis advisor Dr. Shaikh Abdur Razzak for his excellent guidance, inspiration and motivation. I am very thankful for his support academically and emotionally. I would like extend my deepest gratitude to my thesis co-advisor Dr. M. Mozahar Hossain for his insightful comments and his encouragement gave me the power to move on and face all difficulties during this research. I would like to express my deepest gratitude for my advisor and co-advisor for their patience with me and for believing in me. I also wish to extend my sincere gratefulness to my Committee members: Dr. Sulaiman S. Al-Khattaf, Dr. Mohammed Ba-Shammakh and Dr.Saad A. Al-Bogami. Last, I am very thankful to my mother who endured a lot during this period and who believed in me when I did not. My deepest thanks goes to my late father who was the main reason for me to continue my graduate studies. I would like to extend my thanks to my brother, friends, extended family and the (KFUPM) Egyptain society for their constant support.

Table of Contents

LIST OF FIGURES

LIST OF TABLES

ABSTRACT

Full Name : AHMAD HASSAN ALI AL-RASHIDY

Thesis Title : HYDROCRACKING OF VACUUM GAS OIL USING Fe, Ni AND Mo BASED DISPERSED CATAYST

Major Field : MASTER OF SCIENCE

Date of Degree : December 2015

The promotional effects of oil-dispersed slurry catalyst(s) on hydrocracking of heavy oil (vacuum gas oil –VGO) has been investigated. In this regards, an oil soluble bimetallic Ni-Mo and two water soluble bimetallic Ni-Mo and Fe-Mo dispersed catalysts are synthesized, characterized and evaluated. The hydrocracking of VGO experiments are conducted in a batch autoclave reactor at 4 MPa and different temperatures (400-430 °C) without and with presence of a solid hydrocracking catalyst. The product analysis indicates that the water soluble bimetallic catalysts give higher VGO conversion than that of the oil soluble bimetallic catalysts. However, the oil soluble catalyst provides higher yields of gasoline and kerosene fractions (51.96 wt%) than those of the water soluble catalysts (44.79 wt%). The oil soluble bimetallic catalyst is further evaluated as co-catalyst with a commercial Ni-W/Al_2O_3-SiO_2 catalysts. The addition of the oil soluble dispersed catalyst decreases the coke formation on the solid catalyst significantly (almost 30 %). The SEM images of the spent solid catalysts clearly shows the effects of less coke deposition on the catalysts. The kinetics of the dispersed catalysts assisted VGO hydrocracking is modeled by using a five lumped model. A catalyst deactivation function is used to take into account of the catalyst decay with time. The evaluation of the kinetics model parameters shows that the specific reaction rate of formation of (gasoline + kerosene) is significantly higher than the rate of

diesel formation. This is consistent to the higher yield of gasoline and kerosene in presence of the dispersed catalysts.

In addition to the above, a phenomenological based kinetics models have been developed for hydrodesulfurization (HDS) of dibenzothiophene (DBT) and 4-methyl dibenzothiophene (4-MDBT) using a P_2O_5 modified $CoMo/Al_2O_3$ catalyst. The analysis of the developed model suggests that a Langmuir-Hinshelwood mechanism fits the experimental data adequately. The rate constants for the formation of BP are 6-8 times higher than the rate constants for the formation of CHB. Similarly, the rate constants for the formation of MBP are 3-5 times higher than the rate constants of MCHB formation. These observations indicate that the HDS of the model compounds through the DDS route is several times faster than the HDS through the HYD route. Furthermore, the rate constant for the formation of BP and CHB is about two times higher than the respective rate constant for the formation of MBP and MCHB. The addition of P2O5 favored the DDS pathway over the HYD pathway for both DBT and 4-MDBT.

ملخص الرسالة

الاسم الكامل : أحمد حسن علي الرشيدي

عنوان الرسالة : التكسير الهيدروجيني لل(VGO) عن طريق المحفزات المشتته المصنوعة من الحديد والنيكل وا الموليبدينوم

التخصص : الهندسة الكيميائية

تاريخ الدرجة العلمية : فبراير 2015

تمت دراسة الآثار الايجابية للمحفزات المشتتة الذائبة في الزيوت العضوية على التكسير الهيدروجيني لل (VGO). في هذا الاطار تم تحضير ومعرفة خصائص وتقييم نوع من المحفزات المشتتة القابلة للذوبان في الزيت العضوي و يحتوي المحفز على النيكل والموليبدينوم ونوعان اخران قابلان للذوبان في المياه يحتوي الاول على الحديد والموليبدينوم و الثاني على النيكل والموليبديوم. تم اجراء التكسير الهيدروجيني لل (VGO) في مفاعل من النوع batch autoclave reactor عند ضغط 4 ميجا باسكال وعند درجات حرارة مختلفة تتراوح من 400 ل 430 درجة مئوية في وجود وعدم وجود محفز تكسير هيدروجيني صلب. يشير تحليل ناتج التجربة إلى أن المحفزات ثنائية المعدن القابلة للذوبان في الماء تعطي تحويل أكبر لل (VGO) مقارنة بالمحفزات ثنائية المعدن القابلة للذوبان في الزيت. إلا أن المحفزات ثنائية المعدن القابلة للذوبان في الزيت تعطي نسب أكبر من الجازولين والكيروسين (51.96 wt%) مقارنة بالنسب الناتجة عن المحفزات القابلة للذوبان في الماء وهي (44.79 wt%). تم تقييم المحفز ثنائي المعدن القابل للذوبان في الزيت كمحفز مساعد للمحفز التجاري **Ni-**W/Al2O3-SiO2. إضافة المحفز المشتت القابل للذوبان في الزيت تقلل من معدل تكون فحم الكوك على سطح المحفز الصلب بنسبة 30%. صور ال SEM للمحفز الصلب المستهلك تظهر بوضوح تأثير إنخفاض معدل ترسب فحم الكوك على سطح المحفز. تمت نمذجة حركية تفاعلات و ميكانيكيات التكسير الهيدروجيني الذي تم بمساعدة المحفزات المشتتة باستخدام النموذج الخماسي المجمع **five lumped model**. تم اضافة دالة تعطيل المحفز للنموذج لأخذ تردي حالة المحفز مع مرور الوقت في الاعتبار. تقييم عوامل نموذج التفاعل يوضح أن معدل تكون (الجازولين + الكيروسين) أكبر من معدل تكون الديزل. وهذا يتفق مع زيادة نسبة تكون الجازولين والكيروسين المحفز المشتت.

بالإضافة إلى ما سبق تم تطوير نماذج لميكانيكيات التفاعلات **phenomenological based kinetics models** للتفاعلات الهيدروجينية لنزع الكبريت (HDS) لل (DBT) و لل(4-MDBT) باستخدام المحفز CoMo/Al2O3 المعدل ب P_2O_5. تحليل النموذج المطور يشير إلى أن آلية لانجمير-هنشلوود يناسب البيانات التجريبية على نحو

كاف. ثوابت معدل تكوين ال BP أعلى 6-8 مرات من ثوابت معدل تكوين ال CHB. وبالمثل، فإن ثوابت معدل تكوين ال MBP أعلى 3-5 مرات من ثوابت معدل تكوين ال MCHB. هذه الملاحظات تشير إلى أن العملية الهيدروجينة لنزع الكبريت HDS لمركبات النموذج من خلال عملية نزع الكبريت المباشرة DDS أسرع عدة مرات من العملية الهيدروجينة لنزع الكبريت HDS من خلال الهدرجة HYD. وعلاوة على ذلك، فإن ثابت معدل تكوين ال BP وCHB هو أعلى بحوالي مرتين من ثابت معدل تكوين ال MBP وMCHB. إضافة ال P_2O_5 أعطت الأفضلية لعملية نزع الكبريت المباشرة DDS مقارنة بعملية نزع الكبريت بالهدرجة HYD لكلا من ال DBT و 4 MDBT.

CHAPTER 1

INTRODUCTION

The trends for saving energy, conservation of resources and clean energy are rising in the last decade because of the depletion of fossil fuel resources. The International Energy Agency (IEA) has setup two scenarios, the Current Policies Scenario and the New Policies Scenario. The Current scenario deals with the polices implemented by governments and the New scenario deals with board polices that take into account global warming, renewable energy, programs related to nuclear powers and etc[1]. Figure 1-1 shows the prediction of these two scenarios on the energy demand by source, it's very clear that fossil fuels are the major source of energy [1].

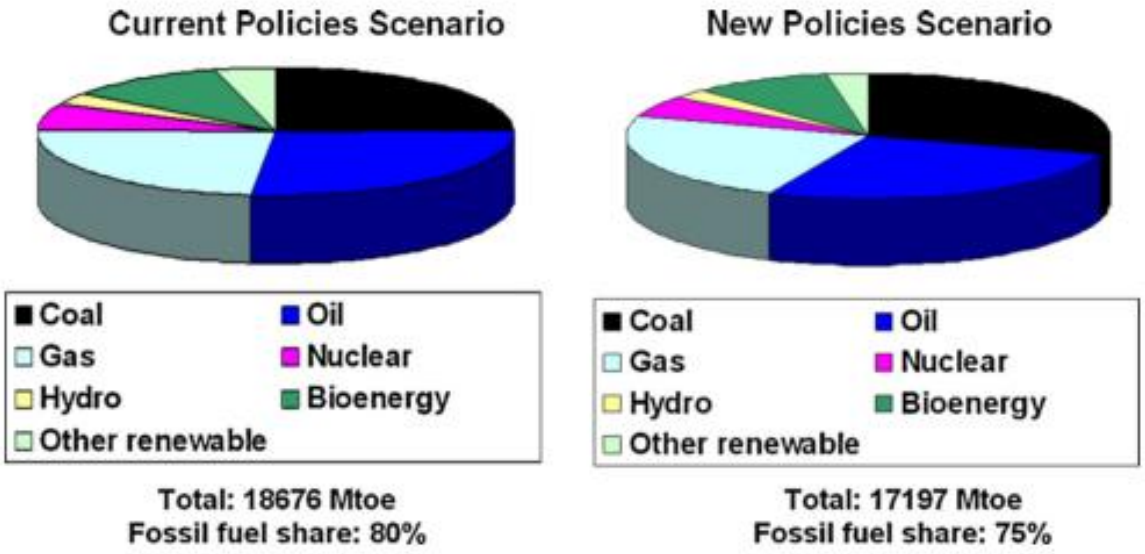

Figure 1-1 Energy requirements: scope at 2035

Fossil fuels is the major source of energy now and in the future. However, its conventional sources are being depleted. Therefore exploitation of unconventional sources like heavy oils, ultra heavy oils, tar sand and oil shale is a must.

The demand for light hydrocarbons and transportation fuels is increasing, therefore heavy feeds and residues should be converted into light fuels. This can be accomplished by using thermal cracking or hydrogen pressurized thermal cracking (hydro cracking) processes. Cracking is the process of breaking heavy hydrocarbons into lighter ones by using heat with the presence of a catalyst. Some of the frequently used catalysts in the industry are Mo, Co, Ni and W oxides which are supported on a alumina matrix, silica matrix or a mixture of silica/alumina matrix[2].

Gasoline is one of the most important products of the petroleum industry. Gasoline is a mixture of light hydrocarbons originate from different streams in the refinery as shown in Figure 1-2 [3].

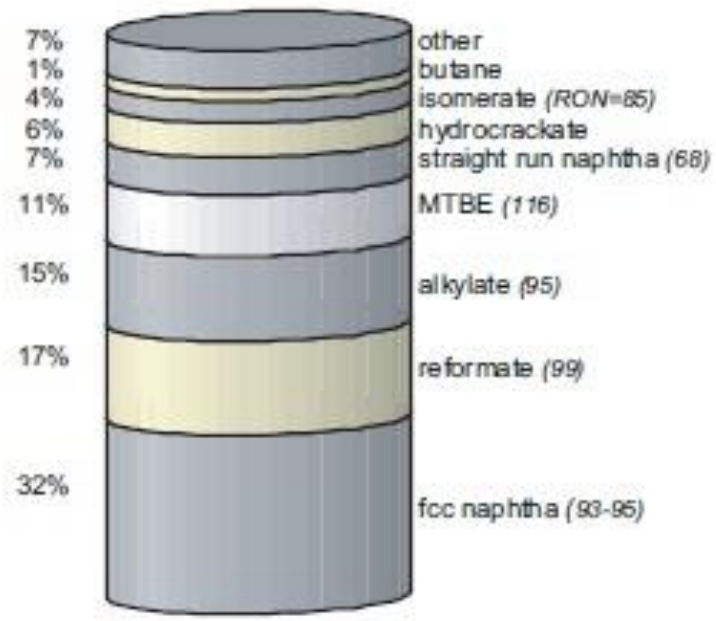

Figure 1-2 gasoline composition

The main component of gasoline is naphtha; naphtha is a product produced by distillation of crude oil and cracking of the higher hydrocarbons [3].

Cracking is converting hydrocarbon compounds with large molecular weights into hydrocarbon compounds with lower molecular weights under high temperatures with the aid of a catalyst. The main two catalytic cracking processes are the fixed bed process and the moving bed process like Fluidized Catalytic Cracking and Slurry Phase hydro cracking with dispersed catalyst. Many processes were developed in order to overcome problems like cocking that frequently occurs during any catalytic cracking process [3].

Dispersed catalysts were first used in 1913 to convert coal into liquid fuels under hydrogen pressure, after that dispersed catalyst was linked to heavy oil upgrading [4]. Dispersed catalysts are commonly utilized in the slurry bed technology. The technology was first used in Germany to convert coal to oil, after that when oil supplies were limited

the technology was used to handle crude oil. Lately the technology was reformed to treat vacuum residue feeds.

The contribution of this Thesis is categorized into three main parts:

- Two water soluble bimetallic and an oil soluble bimetallic precursors are developed and studied for the (H.C) of VGO. Results show that the oil soluble bimetallic precursors give the best results in terms of liquid yield while inhibiting coke formation.

- Hydrocracking of VGO is conducted in the presence of a solid (H.C) catalyst and an oil bimetallic dispersed catalyst as co-catalyst. Results show that using this method causes a significant decrease in the coke formed on the solid catalyst surface.

- A five lumped kinetic model is devolved to study the kinetics of the (H.C) of VGO in the presence of a solid (H.C) catalyst and an oil bimetallic dispersed catalyst as co-catalyst.

CHAPTER 2

LITERATURE REVIEW

2.1 Cracking Processes

Fixed bed process, moving bed process, ebullated bed process and slurry bed process are the main four types of processes used in the industry and being studied in general. Until March 2003 there were 73 hydroprocessing units in the world. About 60 of these are fixed bed reactors, 12 are moving and ebullated bed reactors and 1 slurry bed reactor. Fixed, moving and ebullated bed process are more evolved than the slurry bed process which is under development [2].

2.1.1 Fixed Bed Process

The fixed bed reactor is frequently used in the industry for hydroprocessing because it is evolved technically, low cost, stability and reliable performance. The fixed bed reactor can treat feeds with high sulfur content but not feeds with high metal content to prevent deactivation of the catalyst used. The allowed percentage of metal content in the feeds entering the reactor ypically (Ni+V) is < 250 ppm [2].

The main objective of a fixed bed is to hydrotreat heavy fractions, added to that hydrodesulfurization (HDS), hydrodenitrogenation (HDN), hydrodemetallization (HDM) and asphaltene conversion [2].

Heavy oil feeds and residue feeds may contain enough amounts of metals and coke producing molecules, which can deactivate and poison the catalyst increasing the cost of recovery and hence increasing the operating cost [2].

Figure 2-1 shows the usual configuration of a fixed bed reactor. The figure contains a bed of catalyst, a bed guard, a feed distributor and a catalyst support.

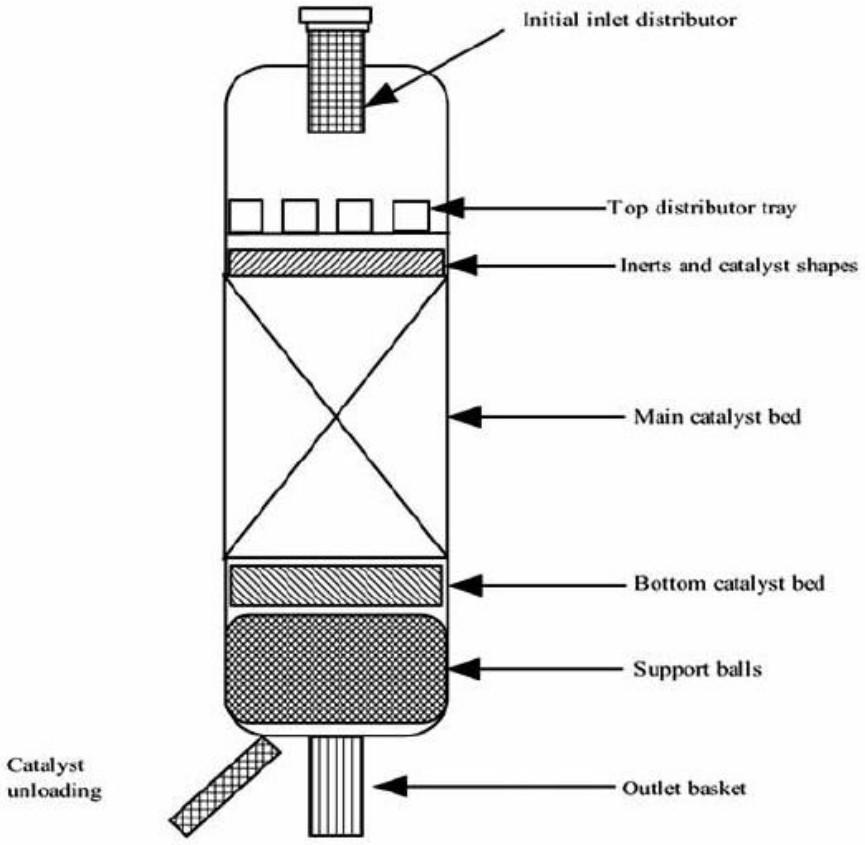

Figure 2-1 configuration of a fixed bed reactor

2.1.2 Moving Bed Process

As mentioned before the only set back of the fixed bed reactor is that it can only deal with feeds with low metal levels. Since the properties of petroleum feeds are changing with

feeds with high metal, nitrogen, asphaltenes and sulfur content, moving beds where the solution for these feeds [2].

It is a general practice in the industry to use one or more moving beds before a fixed bed reactor, this practice is done to reduce contaminants that may plug or cause fouling to catalyst used in the fixed bed. The catalyst is regularly replaced keeping the main reactors always online.

The catalyst used in a moving bed reactor is similar to the catalyst used in a fixed bed reactor, the only difference is the shape of the catalyst used in the moving bed and it is chosen to reduce erosion and to increase the strength of the particle. In the process, the spent catalyst is withdrawn from under the reactor and the newly fresh catalyst is added to the upper part of the reactor, this process is slow accounting for better back mixing of catalyst and feedstock. The moving bed efficiency is considered greater than the ebullated bed and the products produced by the moving bed have a better quality than the products produced by the ebullated bed, this is due to the better back mixing of the catalyst and feedstock. Moving bed reactors are well suited to deal with feeds containing metal content up to 400 ppm [2].

2.1.3 Ebullated Bed Process

There are many problems that arise when a fixed bed has to deal with heavy feeds that contain high amounts of heteroatoms, metals and asphaltenes. A solution to these problems may be to arrange a number of fixed beds in series to obtain high conversion of heavy feed stocks; this solution is very expensive and commercially impractical to some heavy feeds.

The ebullated bed reactors where developed for such heavy feeds with better efficiency and performance [2].

The mixture containing the feed and the hydrogen enter from under the reactor and flow in the upwards direction through the catalyst bed, this causes the bed of catalyst to expand and back mix preventing plugging. The catalyst is not fixed and throughout the process the catalyst is fluidized with the incoming flow of feed. The ebullated bed system is able to convert any heavy feedstock into low sulfur distillates [2].

The significant difference between the ebullated bed and the fixed bed is the ability to add make up catalyst or remove spent catalyst without interfering with the process. This feature is important for processing high metal content feeds and high asphaltene feeds. The design of the bed allows enough space between each particle allowing trapped particles to pass across preventing pressure drop and plugging. The usage of catalyst particles with small diameters up to 1 mm is hence facilitated, this causes an increase in the reaction rate [2].

The catalyst used in the ebullated bed is similar in chemical composition as the catalyst utilized by the fixed bed process and they are both supported [2].

2.1.4 Slurry Bed Process

The slurry bed process involves hydrocracking with a catalyst, pressurized hydrogen and high temperatures. The reaction is thermally driven, meaning that the reaction is mainly thermal cracking. The catalyst and high pressure hydrogen inhibits coke production and causes more valuable products to be produced. The slurry bed process is best suited to lead

with heavy feeds containing high metal content, carbon residue and asphaltene. This process has many advantages like good product selectivity, yield, no plugging, simple flow scheme, flexible operations, high space velocity and conversion rates and is adapted to a wider range of feeds. The main concern is that the slurry bed process is more challenging to operate than other processes [2].

During the process, the feed, the catalyst and hydrogen are mixed before entering the reactor. Throughout the process the catalyst and the feed are well mixed and are kept in suspension. After the process is done the products and the catalyst are separated. The coke formed is deposited on the catalyst surface and is removed with the catalyst therefore no plugging occurs. Solid particles are recovered with the untreated organic fraction and are separated by distillation or solvent deasphalting [2].

Slurry bed process is capable of producing products like gasoline, and diesel fuel or vacuum gas oil. The yield and the selectivity depend on the degree of conversion. Optimum operating conditions are temperatures of 420-460 ^{o}C and pressure about 10-20 Mpa [2].

Slurry process is distinguished by operating with a catalyst that is dispersed in the feed. The size of this catalyst is very small. The reactants and the catalyst are kept in suspension and well mixed in the presence of pressurized hydrogen. The main objective a slurry process operating with a dispersed catalyst is to decrease coke formation. The catalyst is usually a transition metal sulfide (such as Mo, W, Fe and etc). The dispersed catalyst has a higher stability than normal hydrocracking catalysts. Due to the higher satiability of these catalysts, the interaction between the oil and hydrogen is high. The small size of the catalyst enables better catalytic utilization which in turns allows large complex molecules reach

active sites instead of blocking the pores, this leads to less coke formation. Dispersed catalysts are better suited to handle heavier feed stocks over supported hydrotreating catalysts, making slurry processes more capable to deal with difficult feed stocks than any other process [1].

The catalysts utilized in the slurry bed processes are differentiated into three types according to their physical properties: Powder solid catalyst, oil soluble catalyst and water soluble catalyst [2].

Oil soluble and water soluble catalysts are used as non-catalytic precursors that are converted to the catalytic phase before being added to the feed or after their addition during reaction conditions. Whereas the solid powder catalyst where the active phase is a powder is added directly to the feed without any activation steps. For the oil soluble and water soluble catalyst, a solution is made either in oil or water according to the precursor and then added to feed. The feed and the precursor solution are well mixed to ensure better dispersion of the catalyst; Dispersion achieved in this case is better than using solid powders and mixing them directly with the feed. Solid heterogeneous catalysts are added in relatively larger amounts (1-5 wt %) to ensure adequate dispersion, while using oil and water soluble precursors require less concentration (in the order of ppm) to achieve better dispersion. Furthermore, less concentration of water and oil soluble precursors makes them the best choice to overcome increasing cost of catalysts material. The low concentrations of the oil and water soluble precursors are particularly important because the catalysts are trapped in the solids formed and are difficult to recover and hence are lost with these formed solids. The major compounds that are used as oil soluble precursors are mainly organometallic compounds like molybdenum, nickel and iron naphthenates and alkyl

thiometallates. The uses of oil soluble precursors are restricted to 1000 ppm due to the fact that these compounds are costly. Water soluble precursors are a better alternative due to their low cost and easy synthesis. The most common molybdenum water soluble precursors are Phosphomolybdic acid, ammonium molybdates, ammonium heptamolybdate and ammonium tetrathiomolybdate [5].

2.2 Industrial Applications of Slurry Hydrocracking

Slurry hydrocracking was first employed and used in Germany in 1929 to produce oil from coal, then as oil resources become limited the process was modified to treat crude oil. There are a number of industrial process that use slurry technology like VCC, SRC Uniflex^{TR}, Soc, $(HCAT/HC)_3$, HDH/HDHPLUS and EST [2].

2.2.1 Veba Oel's Combi-Cracking (VCC) Process

The same concept used for the Bergius hydrogenation technology in Germany was used in the VCC process. A unit was built at Bottrop refinery by Veba in 1983 and the unit was later reformed to operate on vacuum residue in 1988. During the process, solid powder additive are added to the residue and kept in suspension with the presence of H_2. Solid powdered of Bayer red mud or lignite was used. The reactor used was operated at 440-485 °C, 15-30 MPa and upward flow scheme. The conversion of the residue was proclaimed to be 95% or above[1], [2].

2.2.2 PetroCanada's SRC Uniflex^{TM} Process

The UOP Uniflex process is the result of merging certain elements from the Canmet process and the Unicracking and Unionfining process technologies (UOP). Figure 2-2

shows a simplified scheme of the Uniflex process unit. In this process flow diagram separate heaters are used to heat the gas which is recycled and the liquid feed to the specified temperature. The outlet streams of the heaters enter the slurry reactor from the bottom section. The outlet stream of the reactor is subjected to quenching to stop further reactions and then allowed to enter a series of separators where, the gas produced is recycled back to the reactor. A fractionation section is utilized to recover naphtha, light ends, diesel, vacuum gas oil and unconverted feed from the liquids produced of the separators. Part of the heavy vacuum gas oil is recycled back to the reactor. The reactor of the UOP operates at mild conditions (435-471°C and 138 bar)[1], [2], [6]–[8].

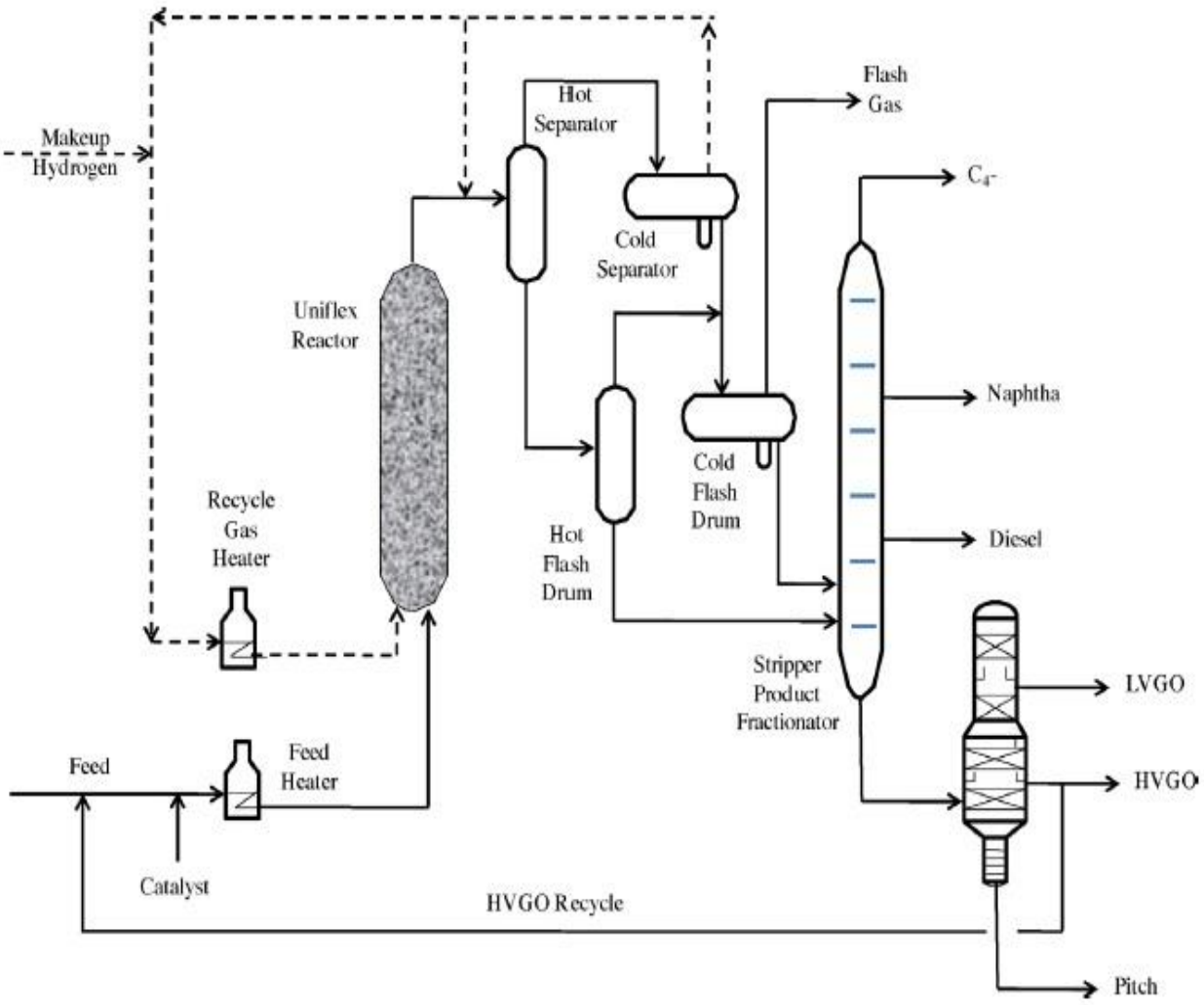

Figure 2-2 Uniflex process flow scheme [8]

2.2.3 Intevep's HDH/HDHPLUS Process

The Venezuelan INTEVEP company began the HDH process for converting heavy residues and oils. The process utilizes an inexpensive natural occurring ore as a catalytic additive; it boosts hydrogenation and decreases coke formation. 2-5wt% is added to the process and mild operating conditions are used, 7-14 MPa, 420-480 °C. A pilot plant was built and 90% conversion was achieved for a number of heavy oils, despite the relatively high conversion an arduous separation process is needed to recover the spent catalytic additive. INTEVEP, IFP and AXENS Company improved the HDH process and named the new process “HDHPLUS”. This process is capable of treating feedstocks and residues with high degree of contaminates[1], [2].

2.2.4 Asahi's Super Oil Cracking (SOC) Process

Asahi Chemical Industries, Nippon Mining Company and Chiyoda Co. developed the Asahi’s Super Oil Cracking Process(SOC). The major aspects of this process are: Minimum amount of the dispersed catalyst is used, a tubular reactor is utilized, high temperatures (475-480 °C), high pressures (20-22 MPa), conversions of 90% are achieved and short residence time. The catalyst used consists of two elements: a transition metal Molybdenum and a fine carbon black particle. Carbon black decreases the coke formation whereas the molybdenum has an important role in hydrogenation. The coke yield reported is about 1wt% when the conversion is 90% [2].

2.2.5 EniTechnologie's EST Process

Snamprogetti and EniTecnologie, companies of the Eni group developed the Eni Slurry Technology (EST) process. Figure 2-3 shows a simplified PFD of the process. The process achieves 95% or higher conversion of the heavy feedstock and high levels of product upgrading. The process can handle heavy crudes, vacuum residues, extra heavy feeds and bitumens from oil sands [1], [8].

The process consists mainly of a hydrotreating reactor where heavy feedstock is processed under mild conditions (410-420°C and 160 bar). The hydrotreating process is conducted in the presence of molybdenum based catalyst and is finely dispersed in the feedstock; usually the concentration of the catalyst does not exceed several thousand ppm. The catalyst facilitates upgrading reactions like desulfurization, denitrogenation, metal removal and reduction of the carbon residue [2], [8].

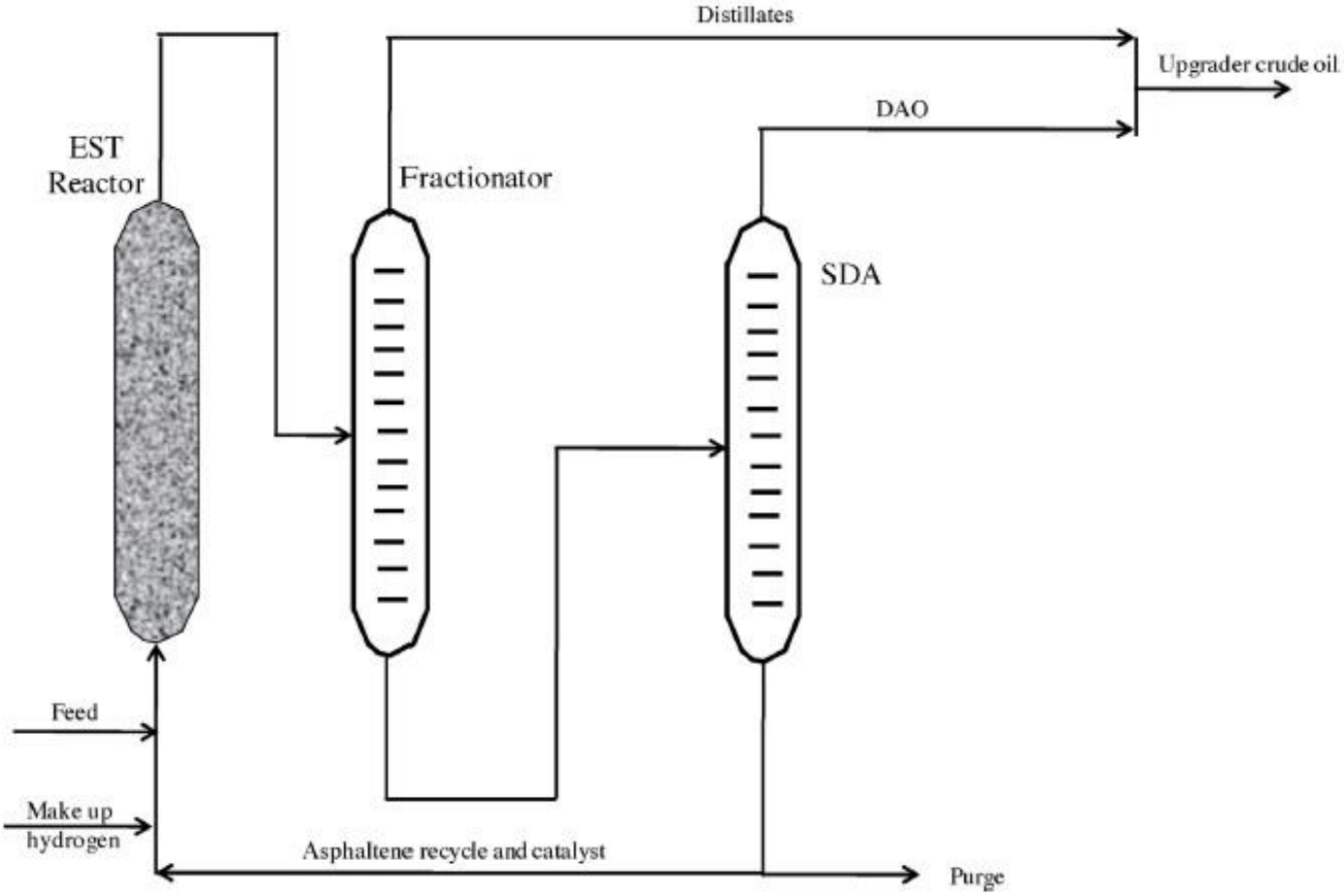

Figure 2-3Simplified PFD of the EST process (ENI) [8]

2.3 Catalyst

2.3.1 Solid Powder Catalyst

The most common metals that are used as solid powder which are added and mixed with the feed are mainly iron, nickel and vanadium. Most industrial processes that take benefit of finely dispersed solid catalyst are once through process that means the catalyst is wasted with the solids formed; this makes the upgrading process in most cases unacceptable [2].

The powered solid catalysts were generally used in the developing stages of the slurry bed technologies like VCC, Canmet and HDH industrial technologies, the main ingredients used in these processes contained $FeSO_4$ additives, natural ore and pulverized coal; the catalyst used is inexpensive and has low catalytic activity, so only less amounts are used to reach a certain degree of activity. Hence, the main drawback of the processes using solid powder catalyst is the elimination of the unconverted residue with the spent catalyst [2].

Breaden *et al.* used a solid catalyst containing a metal phthalocyanine and a particulate iron component. Iron oxides, iron sulfides or mixtures of both are used as the iron component [2].

Finely divided fly ash was used by Khulbe *et al.* as a powder catalyst to decrease coke precursor and hence decrease coke formation [2], [7].

Coal like lignite, bituminous, sub-bituminous can be coated with metal salts such as cobalt, molybdenum and iron, as suggested by Fouda *et al.* The coal particulates should not exceed a certain size, they should be less than 60 meshes [2].

A process that uses an iron petroleum coke catalyst was suggested by Jain *et al.* The iron petroleum coke catalyst was made by crushing coke grains and particles of an iron compound. The catalyst was added to the feed in an amount of 5% by weight [2].

In a recent study by Y.G. Hur *et al.* a heterogeneous solid dispersed catalyst was prepared and used for the hydrocracking of vaccum residue. The catalyst was made of nanosheeet structured WS_2 . The catalyst was prepared by sulfiding tungsten oxide nanorods and the length of the sulfidation time yielded two types of WS_2 nanosheets single or multi layer. The tungsten oxide nanorods were prepared by decarboxylation of tungsten hexacarbonyl in a dispersed state over oleyamine surfactants [9].

H.-J. Eom *et al*. used a Cs-exchanged phosphotungstic acid as a heterogeneous unsupported catalyst for hydrocaraking of extra-heavy oil. Phosphotungstic acid is a heteropolyacid, heteropolyacid is a super acid solid, it can be used as an unsupported acid catalyst. The proton form of heteropolyacids is very soluble in polar organic solvents and water but they cannot be used because of their lower surface area. However, if a portion of the protons are substituted with monovalent ions like Cs+, heteropolyacids are transformed into insoluble salts. These insoluble salts can now be used as heterogeneous unsupported catalysts. Furthermore, as the surface increase more protons are substituted [10].

2.3.2 Oil Soluble Catalyst

Certain materials can be used as oil soluble precursors that can be homogeneously dispersed in the residue and aid more contact between H_2 and the residue. Mainly these materials are organometallic compounds; most commonly used oil soluble precursors are

naphthenates of molybdenum, cobalt, nickel and iron. Some of the common oil soluble catalyst used in the industry are presented in Table 2-1.The precursor is treated before or during reaction conditions after being added to the feed to form the active phase, the active phase is the metal sulfide [2].

Table 2-1 Oil Soluble Dispersed Catalyst for Slurry Bed Process [2]

Licenser	Catalyst components	Feed	Amount of catalyst	Result
Exxon Research and Engineering Co.	Molybdenum alicyclic or naphthenate	Heavy oil with CCR>5%	50-200ppm Solid, noncolloidal catalyst	50% reduction of CCR
Alberta Oil Sands Technology& Research Authority	Fe_2O_3 and molybdenum naphthenate	Cold Lake crude oil	50-200ppm Prepared in situ Can be recycled	50% reduction of CCR Coke yield <1%
	Iron molybdenum	Cold Lake crude oil	0.5-2.0wt% Solid particles with low surface area and pore volume	Conversion>50%
	CrO_3 tert-butyl alcohol	Heavy oil with CCR 5-50%	0.1-2.0 wt% Solid chromium-containing catalyst	Conversion of 80-85%
	iron pentacarbonyl or molybdenum 2-ethyl hexanoate	Athabasca bitumen +50% diluent	0.1-0.5 wt% Well-dispersed colloidal particles	Conversion of 90% coke yield of 0.3%
Chevron Inc.	Mo,Ni acetylacetonates or 2- ethyl hexanoate	Athabasca bitumen	50-300ppm Mixture of asphaltene and metal-doped coke Can be recycled	Coke yield is low
	Molybdenum or tungsten salts of fatty acids (C_7 -C_{12})	Arabian crude	300-l000 ppm	Conversion of 80%
Universal Oil Products Co.	Non-stochiometric vanadium sulfide	Wyoming sour crude oil	Well-dispersed colloidal particles 20-100	High Ni,V removal activity
Institut Francais du Petrole	Molybdenum or cobalt naphthenate	Aramco VR Kuwait AR	20-100 ppm	Asphaltene conversion 70-90%

An experiment was conducted where a dual catalyst system was used for hydrocracking of heavy feeds. G. Bellussi *et al*. showed that the conversion increases considerably when an oil soluble metal hydrogenation catalyst and an acid cracking catalyst are present in the reaction at the same time. Conventional Hydrocracking of heavy feeds using only acid catalyst is challenging, especially because of the cocking formation that blocks the catalyst active sites and the deactivation of the catalyst because of the presence of metals in heavy feeds. Furthermore, recycling of unconverted residues in a hydrocracking reactor using acid catalyst causes the catalyst to deactivate faster. The existence of a hydrogenation catalyst and a cracking catalyst would help resolving the problems mentioned [1], [11].

Molybdenum oil soluble catalysts are extensively studied for slurry hydrocracking. Moreover, many researchers studied the effect of another transition metal as a promoter with molybdenum in a simple mixture. G. Bellussi *et al.* studied the effect of different promoter with an oil soluble molybdenum catalyst; they found that the conversion and coke suppression was approximately the same as using a molybdenum catalyst alone [1].

S.G. Jeon *et al.* revealed a new method to prepare an oil soluble bimetallic catalyst from layered ammonium nickel molybdate. The bimetallic catalyst was prepared by coating layered ammonium nickel molybdate ($(NH_4)HNi_2(MoO_4)_2(OH)_2$) with oleic acid. Ammonium nickel molybdate belongs to a group of layered transition metal molybdates called LTM which are recognized by the general formula $(NH_4)H_{2x}A_{3-x}O(OH)(MoO_4)_2$, where A is a transition metal and $0 \leq x \leq 3/2$. The group prepared a Ni-LTM precursor by precipitation from an aqueous solution and then coated with oleic acid to make it soluble in heavy feeds. The catalyst precursor was tested with other monometallic dispersed catalyst and it showed promising results [12].

2.3.3 Water Soluble Catalyst

Oil-soluble catalysts are very expensive although they have excellent dispersion characteristics and good catalytic activity. Whereas, water-soluble catalysts are less expensive but are less reactive than oil-soluble catalysts. In the case of using water-soluble catalysts, pretreatment like emulsion and dehydration are important before using the catalyst in the process [2]. Two of the common compounds used as water-soluble catalysts are ammonium molybdate and phospho-molybdic acid.

For using a water soluble catalyst first the precursor is dissolved in a solution, the solution is then mixed with the feed forming an emulsion. Dehydration is required to remove the water present in the emulsion, after dehydration sulfurization may be done before proceeding to the reaction or during the reaction (instu) [2]. Some water soluble catalysts used in the industry are listed below in Table 2-2.

Table 2-2 Water soluble catalyst used in the industry[2]

Licenser	Catalyst Components	Feed	Amount of Catalyst	Result
Chevron Inc.	Mo, Ni oxide with aqueous ammonia	Athabasca VR 60% VGO 40%	4-10wt% MoO3 with aqueous ammonia to form a mixture	Sulfur, nitrogen and metal removal > 98%
Exxon Research and Engineering Co.	Phosphomolybdic acid ammonium heptamolybdate molybdenum oxalate	Arabian VR or Cold Lake crude oil	0.2-5wt% Solid molybdenum and phosphorus-containing catalyst	Coke yield is low
	Ni and Mo multimetallic catalyst	Arab Light VR	Ratio of Ni and Mo varied from 0.1 to 10	High HDM activity Bulk
	Nickel carbonate ammonium dimolybdate ammonium metatungstate	Low sulfur diesel oil	Bulk multimetallic catalyst	High HDS, HDN activity
Universal Oil Products Co.	Molybdenum, vanadium and iron metal oxide or salt and heteropoly acid	Lloydminster VR	Solid, non-colloidal catalyst Karamay	Conversion 60-65% coke yield <1%
PetroChina Company Limited	Nickel, iron, molybdenum and iron cobalt liquid catalyst	Karamay AR	Highly dispersed multimetallic catalyst	Conversion 80-90% coke yield <1%

H. Luo *et al*. studied the effect of the dispersion of a water soluble catalyst on the slurry hydrocracking of Liaohe vacuum residue. The group used nickel sulfate ($NiSO_4.6H_2O$) and ferrous sulfate ($FeSO_4.7H_2O$) in proportional as precursor for the water soluble catalyst used, they found out that lowering the interfacial tension between the feed and the catalysts solution improves the dispersion of the catalyst leading to smaller size of particles. Higher dispersion of the catalyst leads to better inhibition of condensation and excessive cracking causing less coke formation [13].

H. Ortiz-Moreno *et al.* investigated the effect of temperature, pressure and catalyst precursor on heavy oil upgrading. The group used ammonium heptamolybdate and ammonium tetrathiomolybdate for the water soluble precursors and were activated in *situ* to obtain MoS_2. The study revealed:

1. Using very low catalyst concentration (300 ppm Mo) has the same effect when thermal cracking is operated without a catalyst.

2. Product distribution can be altered by changing the catalyst concentration used or the operating temperate.

2.4 Kinetic modeling

2.4.1 Model description

Lumped kinetic models are often used to model hydrocracking processes. Lumped kinetics are used by dividing the feed stock and the products produced into several lumps

according to their respective boiling point range [14], [15]. These lumps are considered as a single compound with properties determined form the literature.

The model proposed is based on a model used by T.S Nguyen *et al.* [16], [17]. The feed and the products are grouped into lumps distinguished by their boiling point range, every lump is assumed to be a single compound [14]. In the model used, the feed and the products are grouped and defined into six boiling point ranges:

- Gasoline and kerosene (GASO, 30 – 200 °C)
- Diesel (DIST, 200 – 280 °C)
- Unreacted VGO (VGO, + 280 °C)
- Gases which include hydrogen CH_4, C_2H_6, C_3H_8, C_4H_{10}, C_5H_{12} and H_2S (GAS).
- Coke

Assumptions

The following assumptions are presented:

- Uniform catalyst distribution.
- All reactions are of the first order.
- Uniform liquid and gas phases.
- Uniform solid catalyst distribution in the liquid phase.
- All the reactions are assumed to occur in the liquid phase.

- Only reactions between the lumps are considered and they represent the thermal and catalytic reactions.

Reaction network

Figure 2-4 shows a simple figure of the reaction pathways. For simplicity the lump NAPH was neglected form the all reactions involving R and the lump GAS was produced from all other reactions, neglecting the lump NAPH reduces the number of parameters that should be estimated. From the Figure 2-4, the equations representing the model are as follows:

$$VGO + H_2 \overset{k_1}{\rightarrow} DIST$$

$$VGO + H_2 \overset{k_2}{\rightarrow} GASO$$

$$VGO + H_2 \overset{k_3}{\rightarrow} GAS$$

$$VGO + H_2 \overset{k_4}{\rightarrow} Coke$$

$$DIST + H_2 \overset{k_5}{\rightarrow} GASO$$

$$GASO + H_2 \overset{k_6}{\rightarrow} GAS$$

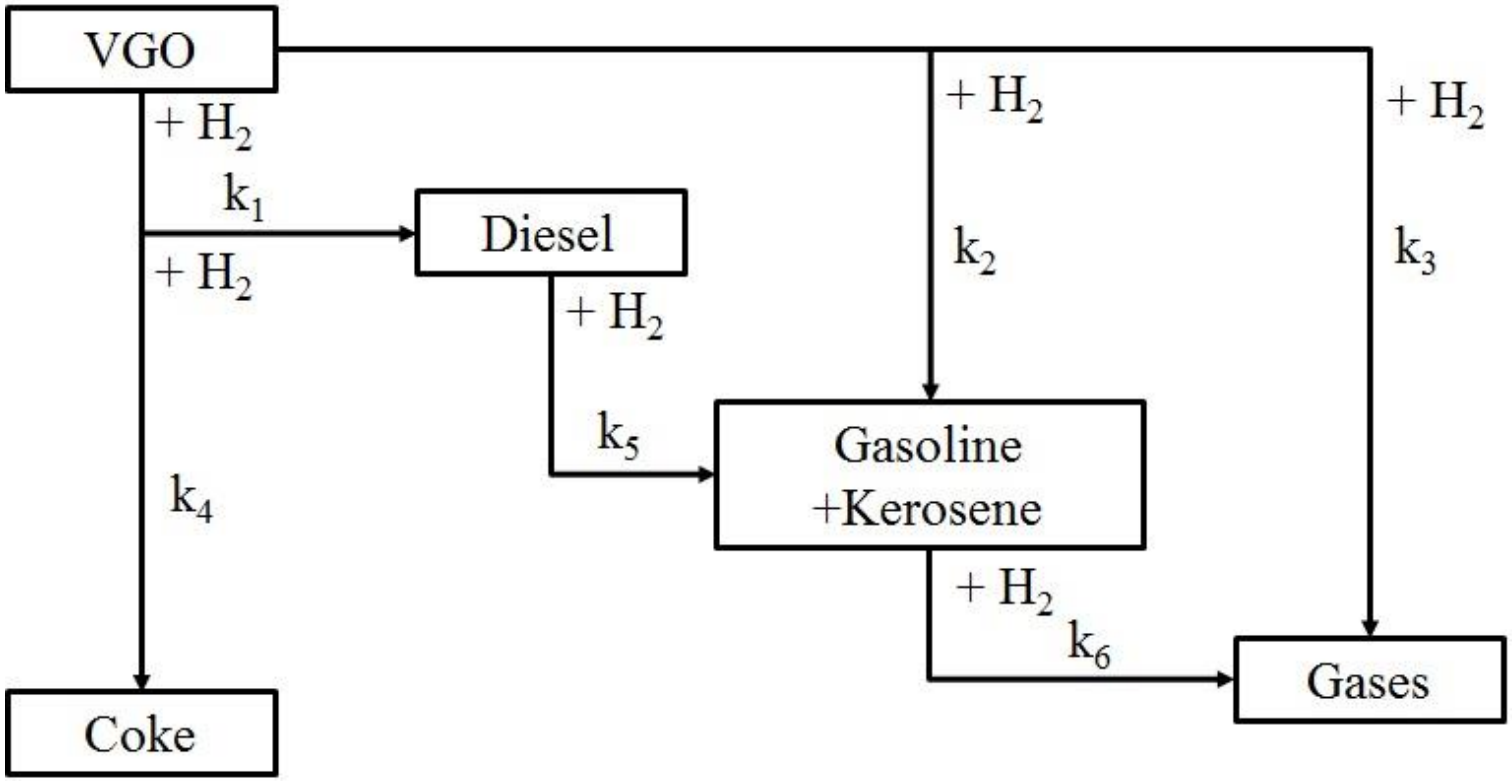

Figure 2-4 Proposed model scheme of the conversion of the heavy residue

2.5 Conclusion of the literature review

The information presented in the introduction and the literature review part can be catagorized by the following:

- Heavy oil upgrading especially hydrocracking processes are very important to make use of the heavy residues that are present and to increase the production of valuable products.

- Slurry hydrocracking is a new technology and has the advantage where coke produced during this process is less than any other process.

- Two types of catalyst are used in the slurry hydrocracking process, oil soluble and water soluble. Research has been done to integrate oil soluble catalysts with the usual industrial supported catalyst but little or no research has been done with the water soluble catalyst integration.

- Lumped kinetic models are best suited to model hydrocracking reaction and are repeatedly reported in the literature.

CHAPTER 3

OBJECTIVE

There are three major objectives in this Thesis project:

1. To develop oil and water soluble dispersed catalysts to minimize the coke formation and enhance liquid products during hydrocracking of heavy oil (VGO).

2. To study the kinetics of the dispersed catalyst assisted VGO hydrocracking.

3. To establish a phenomenological based kinetics model for hydrodesulfurization (HDS) of dibenzothiophene (DBT) and 4-methyl dibenzothiophene (4-MDBT) using a P_2O_5 modified $CoMo/Al_2O_3$ catalyst

Following are the specific objectives:

i. Synthesis of the dispersed catalysts

For the water soluble catalyst (Mo-Fe), a catalyst mixture is prepared by mixing ammonium thiomonomolybdate with nickel nitrate or iron nitrate. For the oil soluble precursors, a bimetallic catalyst is synthesized by precipitating a layered ammonium nickel molybdate from an aqueous solution containing ammonium thiomonomolybdate with nickel nitrate.

ii. Catalyst performance evaluation

The performances of the dispersed catalysts have been investigated in a batch autoclave reactor using vacuum gas oil (VGO) as feedstocks. The reactions are conducted at

temperature ranging from 400 to 430 ℃ and pressure between 7 and 15 MPa. In catalyst evaluation, the following parameters have been investigated:

- Effects of type of water and oil soluble catalyst on coke formation.
- Effect of temperature.
- Effect of residence time.

iii. Characterization of the spent catalyst

The dispersion of the sulfide active phases on the solid hydrocracking catalyst have been studied by Scanning Electron Microscopy (SEM). Furthermore, Fourier Transform Infrared Spectroscopy (FTIR).

iv. Model formulation and Parameter estimation

The kinetics models are developed based on the reaction data and model parameters are estimated using leas square fitting of model parameters using the batch autoclave reactor data implemented in Mathmatica.

CHAPTER 4

EXPERIMENTAL

4.1 Experimental setup

4.1.1 Batch reactor system

Stirred tank reactors are usually selected for batch and semi-batch operation modes for hydrocraking of heavy oils. Figure 4-1 shows a simple flow diagram of the experimental setup. In the figure hydrogen is supplied via the gas cylinders that are directly connected to the reactor. Total mass balance is done by accurately measuring the initial amount of hydrocarbon, the initial amount or flow of hydrogen, the amount of liquid product stream and the amount of the gas product stream. Quantification of the liquid products is done by weighting and gas product quantification needs a flow meter and analysis by gas chromatograph. Gas product stream mainly contains light hydrocarbons, hydrogen sulfide, carbon oxide, nitrogen oxide and unreacted hydrogen [18].

Hydrogen is added continuously from the cylinders for the semi-batch operation mode whereas, in the batch mode the consumption of hydrogen by the reaction is not compensated and the ratio of hydrocarbons to hydrogen is vague after the experiment starts [18].

Batch autoclave reactor is suited best to deal with exothermic reactions. The reactor is suited to conduct experiments with less temperature fluctuations. Important factors like catalyst activity, catalyst selectivity, kinetics of the reactions and catalyst activation energies can be examined and determined by using a batch reactor. In Figure 4-1 a 100 ml

autoclave reactor is utilized. The reactor has a rotor which regulates the stirrer rotations, in-situ sampling port for liquid sampling, gas port sampling, cooling water coils and meters for monitoring temperature and pressure.

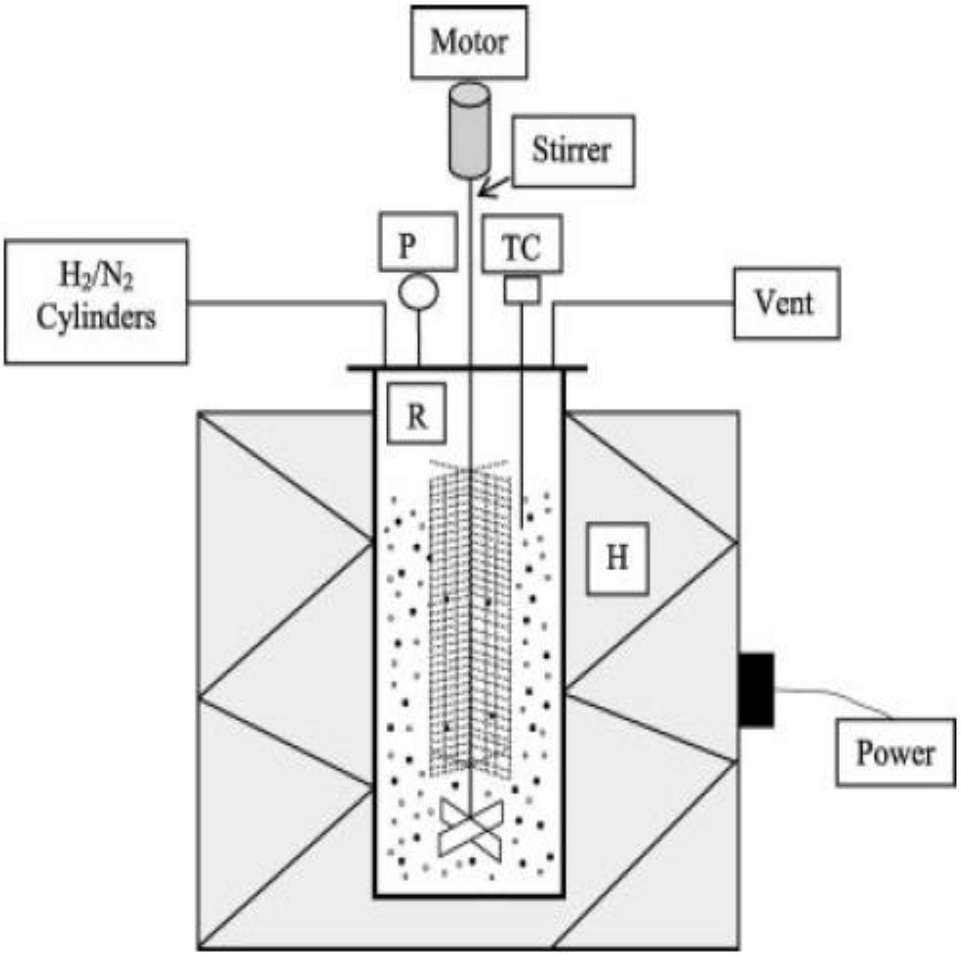

Figure 4-1 Experimental setup of the batch and semibatch process[18]

4.2 Catalyst Preparation

4.2.1 Material

For the water soluble catalyst precursor ammonium thiomonomolybdate, nickel sulfate and iron sulfate was selected. Whereas, for the bimetallic oil soluble catalyst precursor ammonium heptamolybdate ($(NH_4)_6Mo_7O_{24}\cdot 4H_2O$), nickel nitrate ($Ni(NO_3)_2\cdot 6H_2O$), ammonium hydroxide (28.8%,NH_3) and oleic acid was selected and for the solid catalyst a commercial non zeolite catalyst containing nickel, tungsten and alumina was purchased and used. Furthermore, for the feed VGO was selected and obtained from Saudi Aramco.

4.2.2 Synthesis

Water soluble catalyst

In order to obtain 250 ppm of ammonium thiomonomolybdate with 250 ppm of nickel sulfate or iron sulfate, 0.0125g of ammonium thiomonomolybdate and 0.0125g of nickel sulfate or iron sulfate for every 30 g of feed are mixed and dissolved together in 10 ml of water. An emulsifier (Span 80) is then added to the catalyst precursor aqueous solution. The feed is added to a small slurry blender which is maintained at 80°C, after that the catalyst precursor aqueous solution is added drop wise to the slurry blender which is maintained at 80°C and 2000 rpm for about and this producer takes about 20-80 mins. The mixture is then left to be stirred in the blender for 1 hr at 80°C and 2000 rpm. Figure 4-2 show a simpler demonstration of the process. After stirring is complete, the mixture is heated to about 80-180°C and then bubbled with nitrogen to remove the water.

Oil soluble bimetallic catalyst

For preparing the oil soluble bimetallic catalyst ammonium heptamolybdate and nickel nitrate are mixed together in known ratios to get a number of layered transition metal molybdates LTM that are governed by the general formula $(NH_4)H_{2x}Ni_{3-x}O(OH)(MoO_4)_2$ where $0 \leq x \leq 3/2$ as shown in Table 4-1 [19].

Table 4-1 LTM precursors formulas for different Ni/Mo ratios [19]

Ni/Mo	X	LTM precursor
1.5	0	$(NH_4)Ni_3O(OH)(MoO_4)_2$
1.25	0.5	$(NH_4)Ni_{2.5}(OH)_2(MoO_4)_2$
1	1	$(NH_4)HNi_2(OH)_2(MoO_4)_2$
0.875	1.25	$(NH_4)H_{1.5}Ni_{1.75}(OH)_2(MoO_4)_2$
0.75	1.5	$(NH_4)H_2Ni_{1.5}(OH)_2(MoO_4)_2$

The synthesize of the catalyst involved the formation a layered ammonium nickel molybdate precursor, the precursor was prepared by mixing ammonium heptamolybdate ($(NH_4)_6Mo_7O_{24}\cdot 4H_2O$) and nickel nitrate ($Ni(NO_3)_2\cdot 6H_2O$) in a solution with the desired molar ratios mentioned in the table above. Adding concentrated ammonium hydroxide (28.8% NH_3), resulted in the precipitation of a green solid. This green solid dissolves in an excess of ammonia resulting in a deep blue solution. Heat is applied to the solution with constant stirring for 4 hours resulting in the formation of a pale green solid. The solid is filtered, washed and left to dry for 24 hrs at 110°C and 1 atm. The Ni-LTM precursor formed is mixed with oleic acid in excess and stirred with nitrogen. The obtained mixture is left heated at 250°C for an hour; this resulted in a brown color solution. To precipitate

the oil soluble precursor acetone is added to the mixture and the resulted solid is cleaned, washed with acetone to remove any remaining oleic acid and dried.

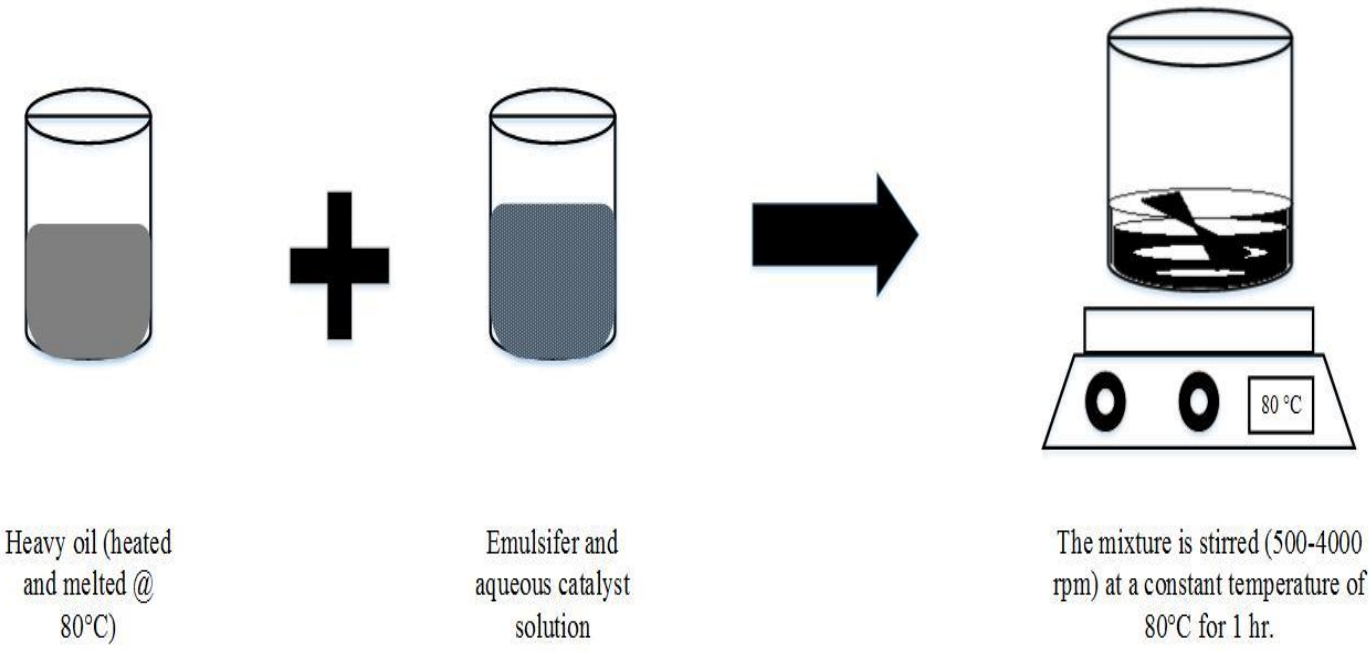

Figure 4-2 Addition of dispersed catalyst and emulsifier mixture to heavy feed oil

4.3 Catalyst characterization

4.3.1 Scanning Electron Microscopy Analysis

SEM analysis is done by Platinum Sputter electron microscope. The catalyst sample is coated with a layer of platinum then placed on a carbon plate. The carbon plate is then inserted in the microscope cell for analysis.

4.3.2 Fourier Transform Infrared Spectroscopy (FTIR)

(FTIR) analysis is done by Nicolet iN10 Infrared Microscope. The sample is finely grounded and pressed into a self-supporting wafer. The wafer is calcined under vacuum at 400 °C for 1 hr. the wafer is then in thr FT-IR cell and then the spectrum is recorded.

4.4 Catalyst evaluation

4.4.1 Experimental procedure

The hydrocracking was performed in a 100 ml autoclave batch reactor. A pressure leak test was conducted before every run. The reactor was pressurized with nitrogen at an initial pressure of 11 MPa, the final pressure was recorded after 1 hr. After the leak test the reactor was purged with hydrogen 3 times to make sure that there is no air left inside to avoid combustion reactions. The feedstock mixture is then prepared as stated in section 3.2.2. The feedstock is charged to the reactor and the reactor is pressurized with hydrogen to 7 Mpa at room temperature. The reactor is then heated to the required temperature; the reaction is then left to proceed for 60 min. After the reaction is complete, the reactor is quenched by increasing the flow of water in the cooling tubes to terminate the reaction immediately. The reactor is then left for two hours to completely cool down to the room

temperature to safely handle it and retrieve the liquid and solid products. Mass balance is done by measuring the weight of the liquid feed and measuring the weight of the liquid and solid products, the closing weight is about 85-90 %. To check the reproducibility of the experimental results, a number of runs were performed, typical errors were in the range of 1 %.

4.5 Manipulation of products after catalyst reaction

4.5.1 Product separation

Liquid and solid samples are recovered in an organic solvent generally THF, toluene, and etc. The mixture is washed with the organic solvent, centrifuged at 12000 rpm for 30 min and finally separated by a Millipore filter. Toluene is used to wash the reactor and the stirrer. The oil and solid products are recovered by washing the solid part that contains the catalyst by n-heptane. The solid part is then dried, weighed and submitted to analysis. If toluene is used, the coke which is insoluble in toluene is separated and extracted with boiling toluene. The isolation of the coke occurs by adding toluene (10:1 by weight) followed by centrifugation at 3000 rpm for 20 min. The previous step is redone once more, consequently filtration is done using a medium size fritted glass, and the solid which is separated is dried at 75°C for 2 hr.

For the gas phase products, the products are collected in a sampling bag and then introduce to a gas chromatograph (GC). Figure 4-3 shows a simple flow diagram of the entire process of hydrocracking using dispersed catalyst.

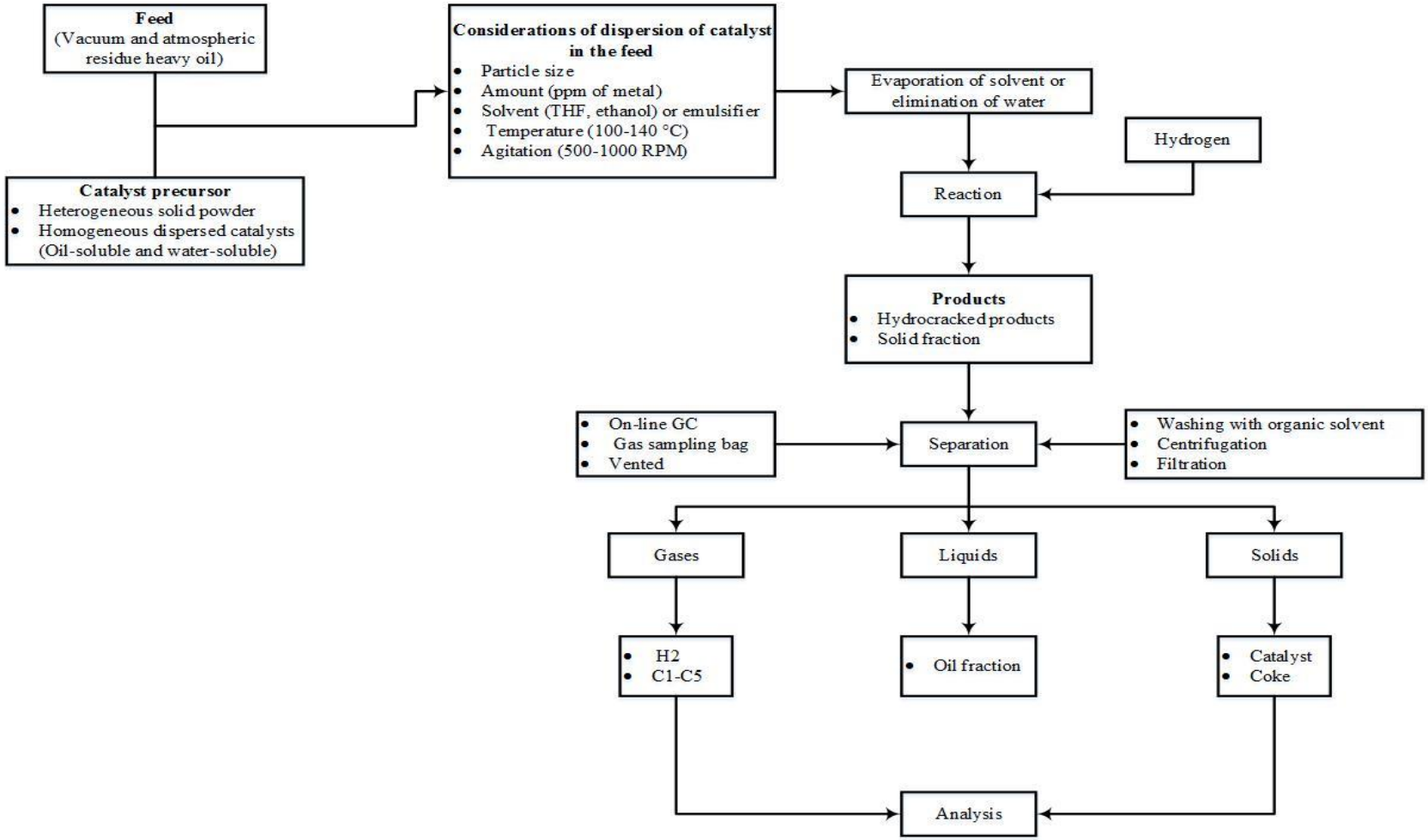

Figure 4-3 Block flow diagram of the hydrocracking process using dispersed catalyst [18]

4.5.2 Product analysis

Gases

Gas products like C_1-C_5 hydrocarbon are identified and quantified using a GC (gas chromatograph).

Liquids

To determine the boiling point range of the liquid products GC temperature simulated distillation (SIM-DIST) and thermogravimetric analysis (TGA) were used.

Spent catalyst

Fourier transform infrared spectroscopy (FTIR) was used with the spent catalyst to ensure that the precursors have been sulfurized in situ during the reaction.

CHAPTER 5

RESULTS AND DISCUSSION

5.1 Hydrocracking of LVGO using different types of dispersed catalyst precursors.

5.1.1 Catalytic activity on different types of precursors

Control experiment (non-catalytic)

A non-catalytic run was conducted as a control to compare the results and the findings of this thesis. The control run was conducted with initial hydrogen pressure of 2.95 Mpa and initial temperature of 25.1 °C. The reaction temperature of 405 °C was reached and maintained after 74 mins. The reaction residence time was 30 mins, at the end of the run the reactor was immediately cooled to room temperature. The conversion was calculated using the following equation:

$$\boldsymbol{Conversion\ of\ LVGO} = \frac{\boldsymbol{W_{LVGOf} - W_{LVGOp}}}{\boldsymbol{W_{LVGOf}}} \times \mathbf{100} \qquad \textbf{(5-1)}$$

Where, W_{LVOf} is the weight percentage of the LVGO in the feed and W_{LVOp} is the weight percentage of the LVGO in the liquid product.The conversion calculated is 55.11 %.

The yield of different products for the control run are presented in Figure 5-1, the gas products distributions for the control run are presented in Figure 5-2 and the temperature and pressure profiles for the control run are presented in Figure 5-3. The product yield (wt%) for different catalyst used are presented in Table 5-1 and the gas distributions (mol%) for different catalyst used are presented in Table 5-2.

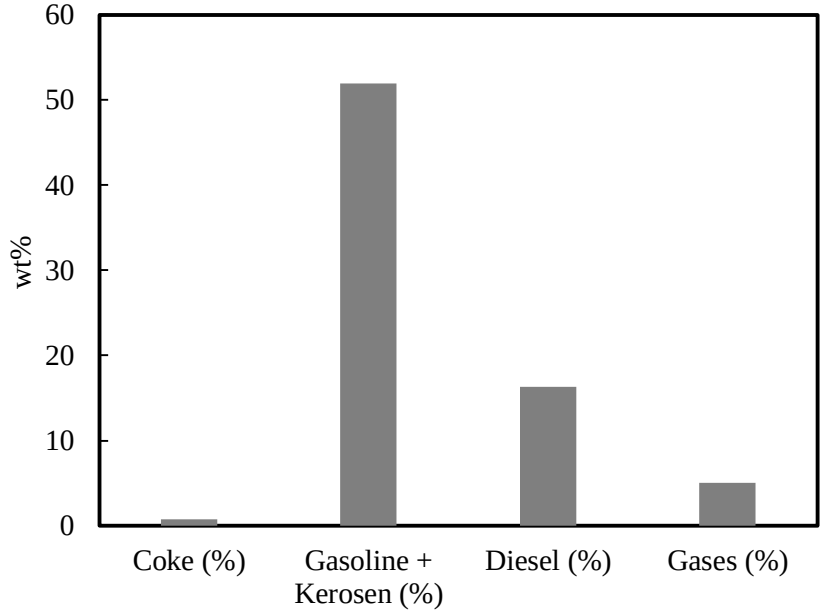

Figure 5-1 Control run product yield wt(%)

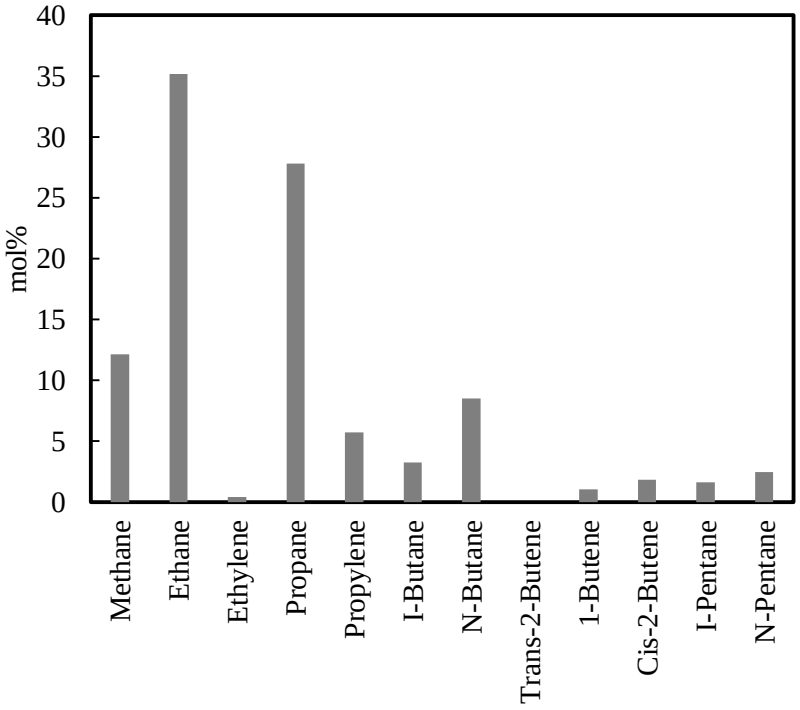

Figure 5-2 Control run gas products yields mol(%)

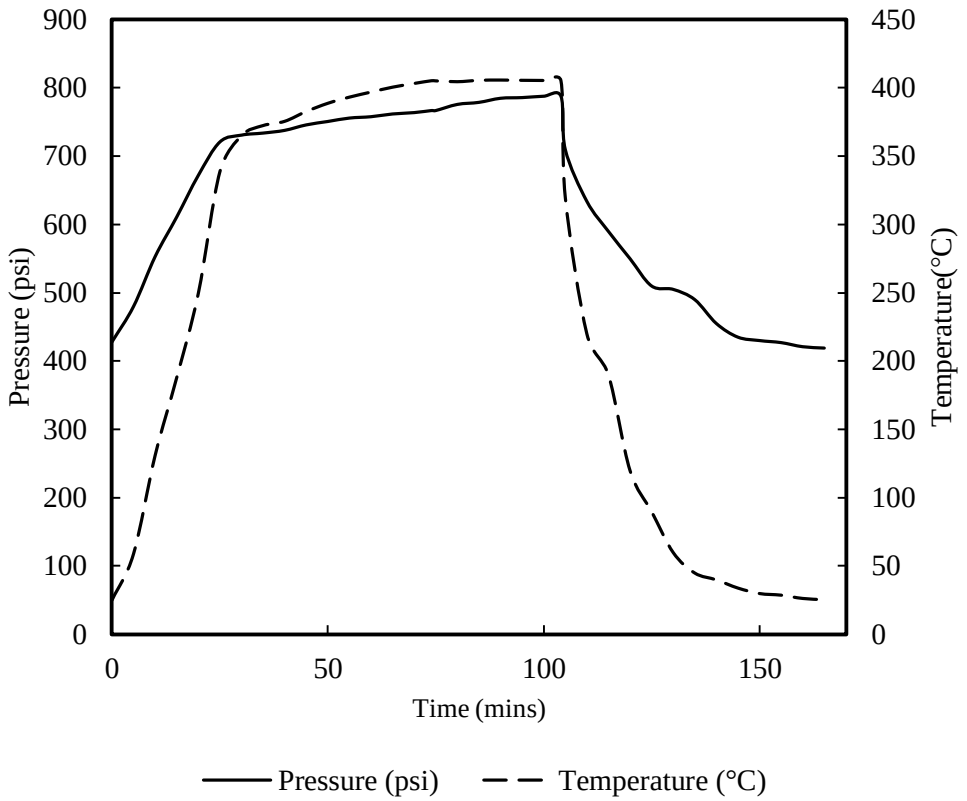

Figure 5-3 Control run pressure and temperature profiles

Table 5-1 Product yield for different catalyst used

	Coke wt (%)	Gasoline + Kerosen wt (%)	Diesel wt (%)	Gases wt (%)
Control Run	0.75	51.97	16.32	5.06
Run(NM)	0.53	44.89	19.52	17.83
Run(IM)	0.46	39.10	11.98	26.49
Run(Ni-LTM)	0.67	51.96	10.74	7.65

Table 5-2 Gas distribution for different catalyst used

	Methane mol%	Ethane mol%	Ethylene mol%	Propane mol%	Propylene mol%	I-Butane mol%	N-Butane mol%	Trans-2-Butene mol%	1-Butene mol%	Cis-2-Butene mol%	I-Pentane mol%	N-Pentane mol%
Control Run	12.16	35.20	0.42	27.82	5.73	3.23	8.50	0.00	1.04	1.81	1.62	2.48
Run(NM)	7.66	58.07	3.20	16.30	3.90	1.80	5.55	0.78	0.68	0.52	1.52	0.00
Run(IM)	5.74	61.32	4.45	13.20	3.54	1.49	5.31	0.00	0.84	1.24	1.00	1.86
Run(NI-LTM)	7.73	59.79	3.68	15.27	3.73	1.52	4.69	0.00	0.67	1.07	0.71	1.14

Nickel Nitrate + Molybdenum Heptamolybdate

Nickel Nitrate and Molybdenum Heptamolybdate (NM) were used as water soluble precursors for the dispersed catalyst, as temperature elevated the precursors were converted to their perspective sulfides. Nickel sulfide and Molybdenum sulfide are the active phases for the dispersed catalyst used. The run was conducted with initial hydrogen pressure of 3.14 Mpa and initial temperature of 23.2 ℃. The reaction temperature of 405 ℃ was reached and maintained after 62 mins. The reaction residence time was 30 mins, at the end of the run the reactor was immediately cooled to room temperature. The conversion calculated by equation 5-1 is 70.12%.

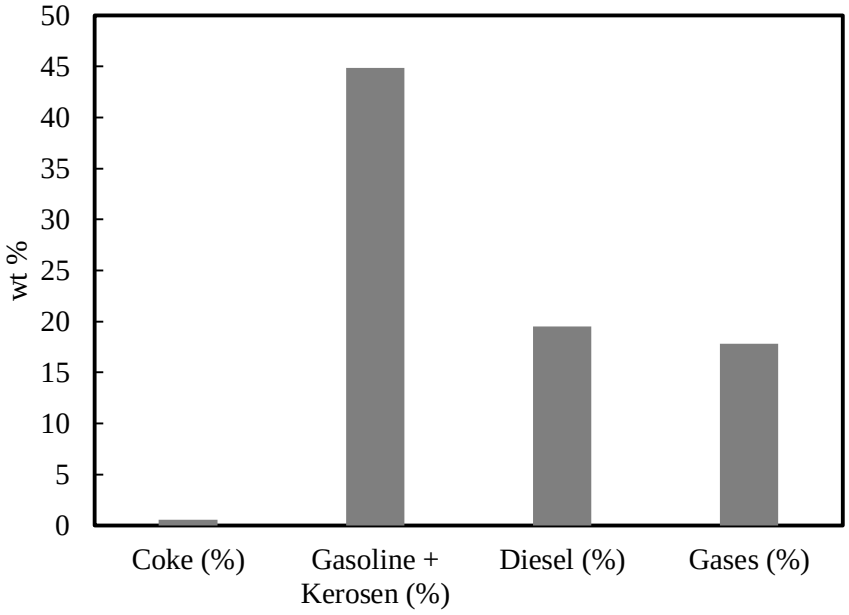

Figure 5-4 (NM) Product yield wt(%)

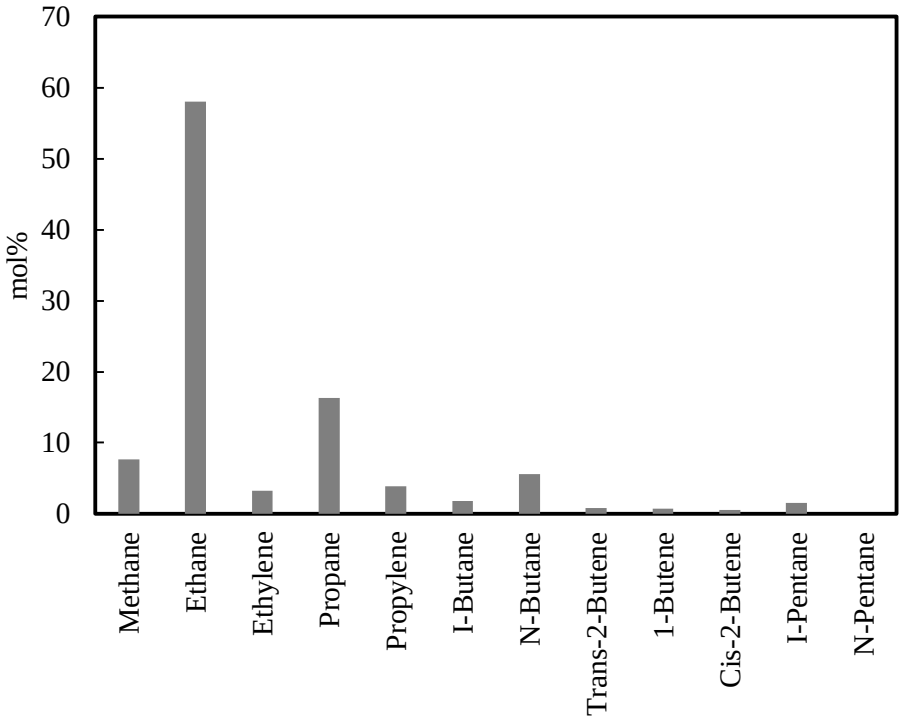

Figure 5-5 (NM) Gas Product distribution

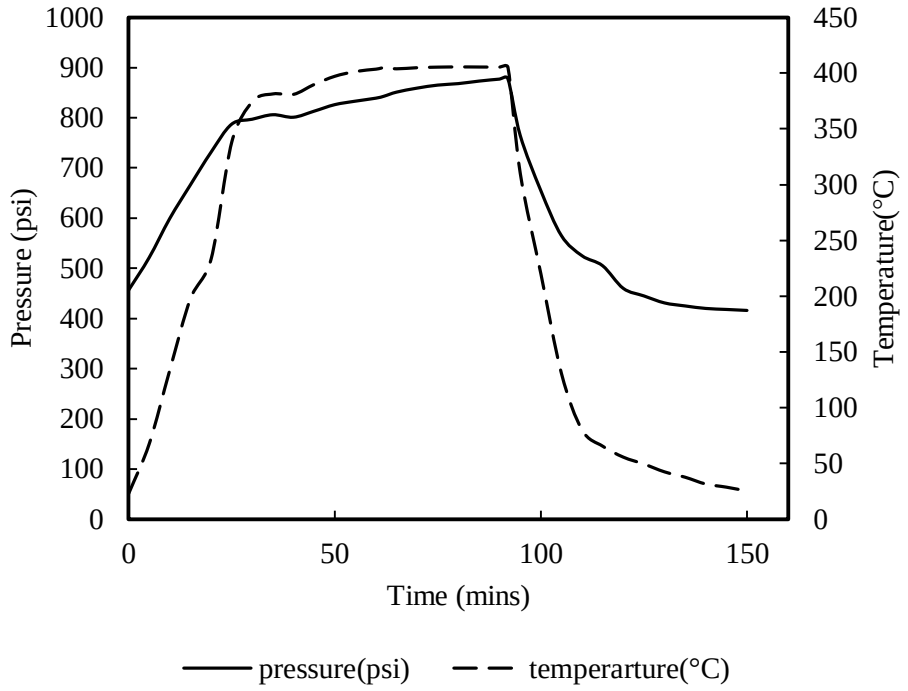

Figure 5-6 (NM) Pressure and temperature profiles

Different products yields for the (NM) run are presented in Figure 5-4, the gas products distributions for the (NM) run is presented in Figure 5-5 and the temperature and pressure profiles for the (NM) run are presented in Figure 5-6.

Comparing the product yields from Table 5-1, it can be shown that adding Nickel Nitrate and Molybdenum Heptamolybdate as dispersed precursor catalyst has a significant impact on the yields of the products. The (NM) run had less yield of gasoline, kerosene and diesel than the control run. Whereas, the gas production was enhanced. Furthermore, the coke production decreased from 0.75 wt% to 0.53 wt%.

Referring to Table 5-2, it can be shown that adding Nickel Nitrate and Molybdenum Heptamolybdate caused an increase in the production of ethane from 35.20 mol% in the control run to 58.07 mol% in the (NM) run. Whereas, all other gases decreased in quantity.

Comparing Figure 5-3 and Figure 5-6, it can be concluded that adding Nickel Nitrate and Molybdenum Heptamolybdate caused an increase in the consumption of hydrogen which justifies the decrease in the coke production, the enhancement in the hydrogen consumption resulted in the increased hydrogenation of the molecules leading to coke formation. Furthermore, the catalyst added did not improve the production of valuable liquid products like gasoline, kerosene and diesel.

Iron Nitrate + Molybdenum Heptamolybdate

Iron Nitrate and Molybdenum Heptamolybdate (IM) were used as water soluble precursors for the dispersed catalyst, as temperature elevated the precursors were converted to their perspective sulfides. Iron sulfide and Molybdenum sulfide are the active phases for the dispersed catalyst used. The run was conducted with initial hydrogen pressure of 3.15 Mpa and initial temperature of 25.8 °C. The reaction temperature of 405 °C was reached and maintained after 47 mins. The reaction residence time was 30 mins, at the end of the run the reactor was immediately cooled to room temperature. The conversion calculated by equation 5-1 is 61.92 %.

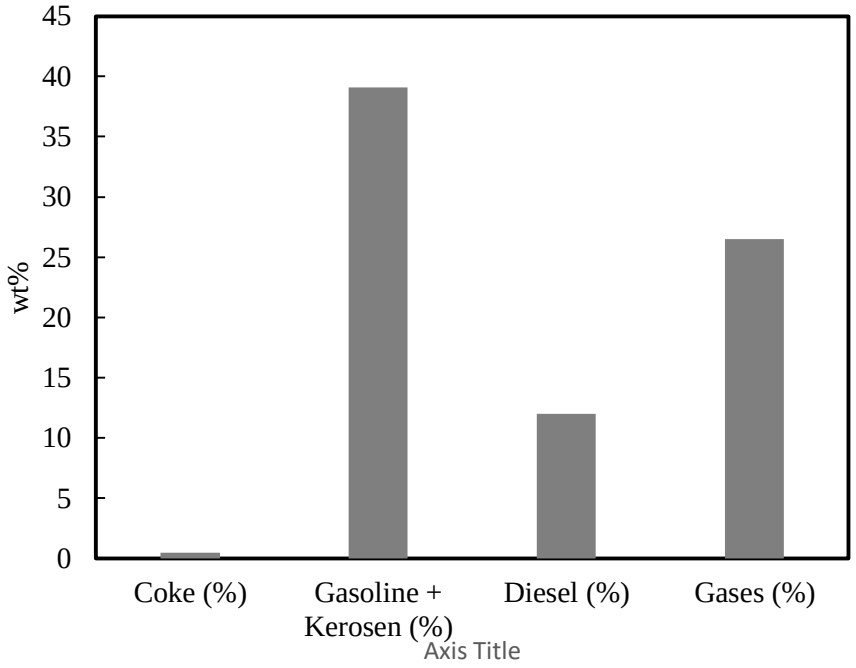

Figure 5-7 (IM) product yield wt(%)

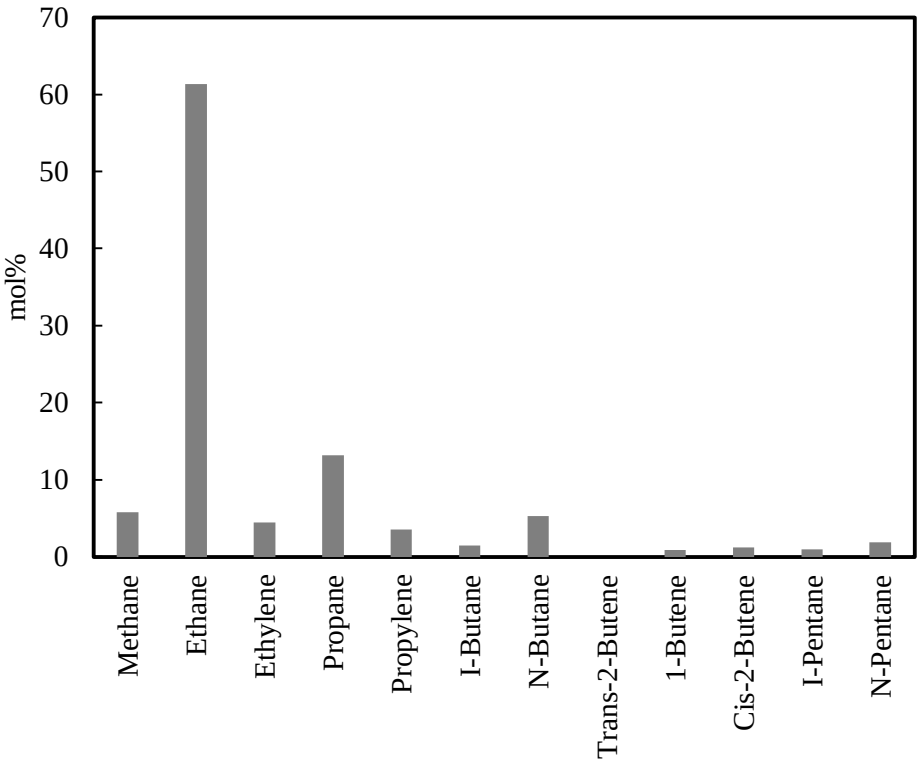

Figure 5-8 (IM) Gas product distribution

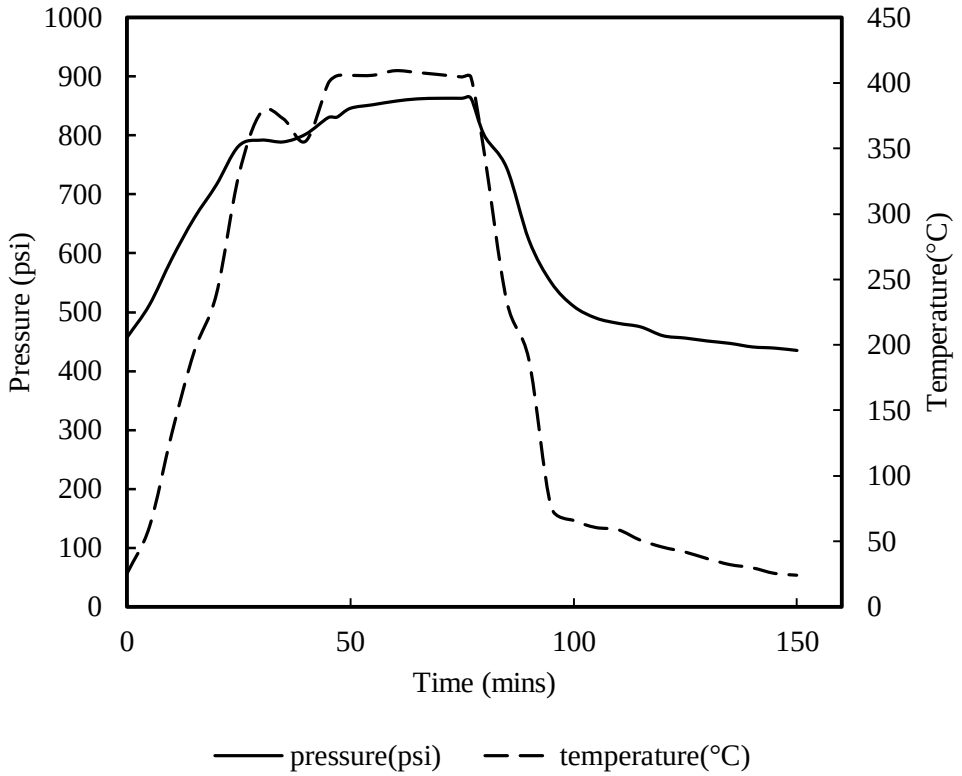

Figure 5-9 (IM) Pressure and temperature profiles

Different products yields for the (IM) run are presented in Figure 5-7, the gas products distributions for the (IM) run is presented in Figure 5-8 and the temperature and pressure profiles for the (NM) run are presented in Figure 5-9.

Comparing the product yields from Table 5-1, it can be shown that adding Iron Nitrate and Molybdenum Heptamolybdate as dispersed precursor catalyst had a significant impact on the yields of the products. The (IM) run had less yield of gasoline, kerosene and diesel than the control run. Whereas, the gas production was enhanced. Furthermore, the coke production decreased from 0.75 wt% to 0.46 wt%.

Referring to Table 5-2, it can be shown that adding Iron Nitrate and Molybdenum Heptamolybdate caused an increase in the production of ethane from 35.20 mol% in the control run to 61.32 mol% in the (IM) run. Whereas, all other gases decreased in quantity.

Comparing Figure 5-3 and Figure 5-9, it can be concluded that adding Iron Nitrate and Molybdenum Heptamolybdate caused an increase in the consumption of hydrogen which justifies the decrease in the coke production, the enhancement in the hydrogen consumption resulted in the increased hydrogenation of the molecules leading to coke formation. Furthermore, the catalyst added did not improve the production of valuable liquid products like gasoline, kerosene and diesel.

Nickel-LTM oleate complex

A layered Nickel metal molybdate (Ni-LTM) was prepared and coated with oleic acid. Thus Ni-LTM oleate complex was used as an oil soluble precursors for the dispersed catalyst, as temperature elevated the precursors were converted to their perspective sulfides. Nickel sulfide and Molybdenum sulfide are the active phases for the dispersed catalyst used. The run was conducted with initial hydrogen pressure of 3.13 Mpa and initial temperature of 24.6 °C. The reaction temperature of 405 °C was reached and maintained after 70 mins. The reaction residence time was 30 mins, at the end of the run the reactor was immediately cooled to room temperature. The conversion calculated by equation 5-1 is 49.78%.

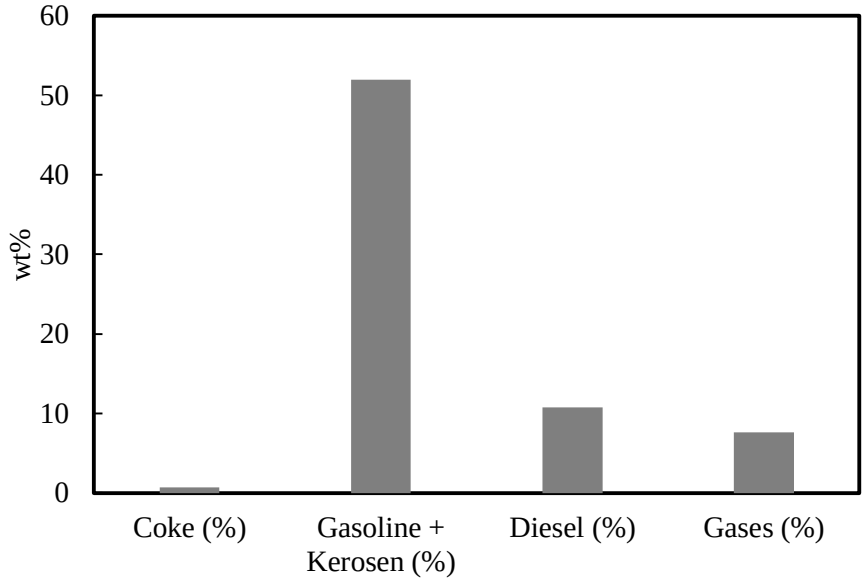

Figure 5-10 (Ni-LTM) product yield wt(%)

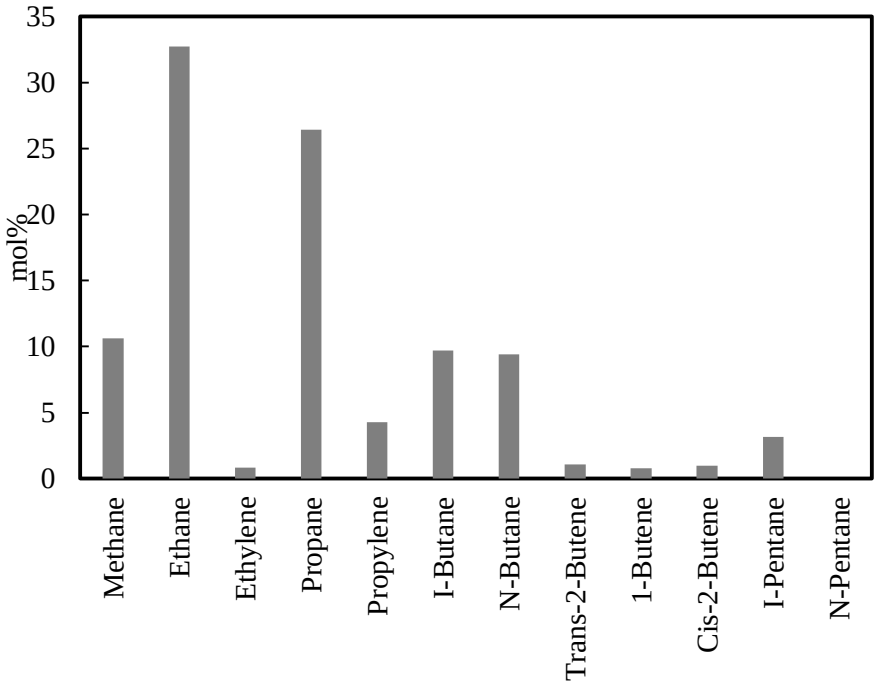

Figure 5-11 (Ni-LTM) Gas product distribution

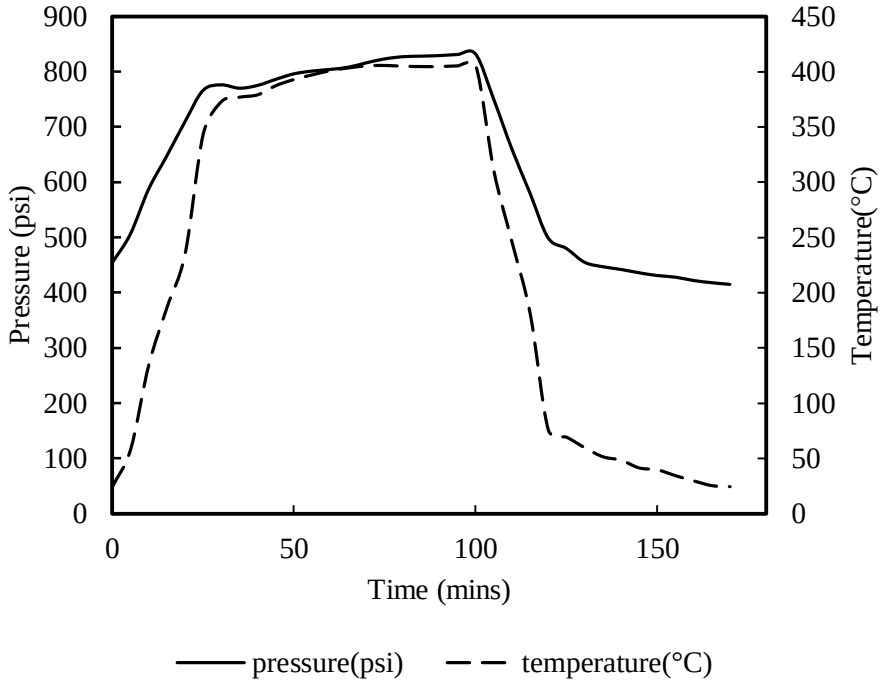

Figure 5-12 (Ni-LTM) Pressure and temperature profiles

Different products yields for the (Ni-LTM) run are presented in Figure 5-10, the gas products distributions for the (Ni-LTM) run is presented in Figure 5-11 and the temperature and pressure profiles for the (Ni-LTM) run are presented in Figure 5-12.

Comparing the product yields from Table 5-1, it can be shown that adding Ni-LTM oleate complex as dispersed precursor catalyst had a significant impact on the yields of the products. The gasoline and kerosene fraction yield was 51.96 wt% compared to that of the control run which was 51.97 wt% which are relatively equal, whereas, the diesel fraction was 10.74wt% compared to that of the control run of 16.32 wt% and the coke yield was 0.67 wt% compared to that of the control run of 0.75 wt%.

Referring to Table 5-2, it can be shown that adding Ni-LTM oleate complex caused an increase in the production of ethane from 35.20 mol% in the control run to 59.79 mol% in the (Ni-LTM) run. Whereas, all other gases decreased in quantity.

Comparing Figure 5-3 and Figure 5-12, it can be concluded that adding Ni-LTM oleate complex caused an increase in the consumption of hydrogen which justifies the decrease in the coke production, the enhancement in the hydrogen consumption resulted in the increased hydrogenation of the molecules leading to coke formation.

Comparing the three precursors used, the Ni-LTM oleate complex had the lowest conversion and the lowest coke reduction but despite that the gasoline and kerosene fraction production was unchanged compared to the control run and the lowest gas production compared to the other two water soluble precursors. Furthermore, the Ni-LTM oleate complex precursor had the highest hydrogen consumption compared to the other two catalysts.

5.1.2 Characterization of the spent catalyst

Nickel Nitrate + Molybdenum Heptamolybdate

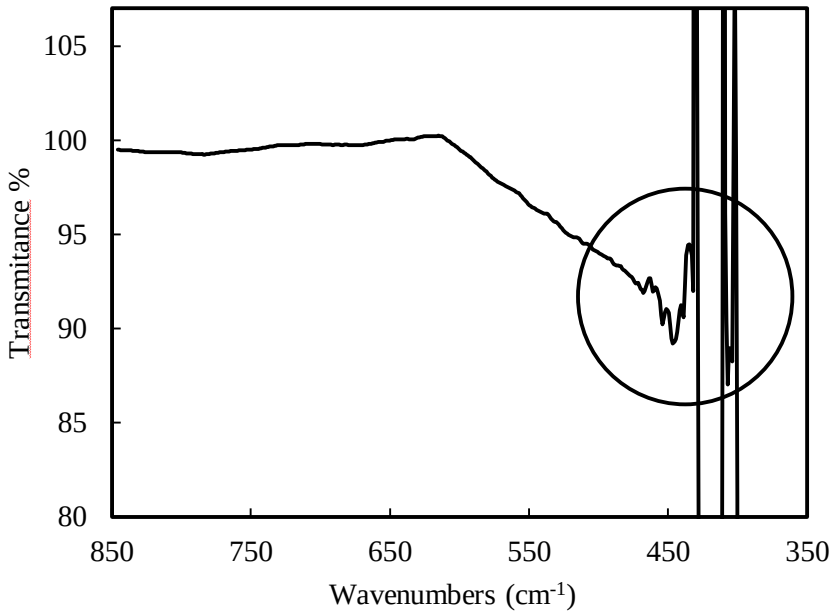

Figure 5-13 NM FTIR spectrum

Figure 5-13 presents the IR spectrum of the spent catalyst of the run conducted with the nickel nitrate and molybdenum heptamolybdate precursors. The presence of peaks in the wavenumbers between 350 and 450 cm^{-1} shows that the precursors have been sulfurized to their active sulfide phase.

Iron Nitrate + Molybdenum Heptamolybdate

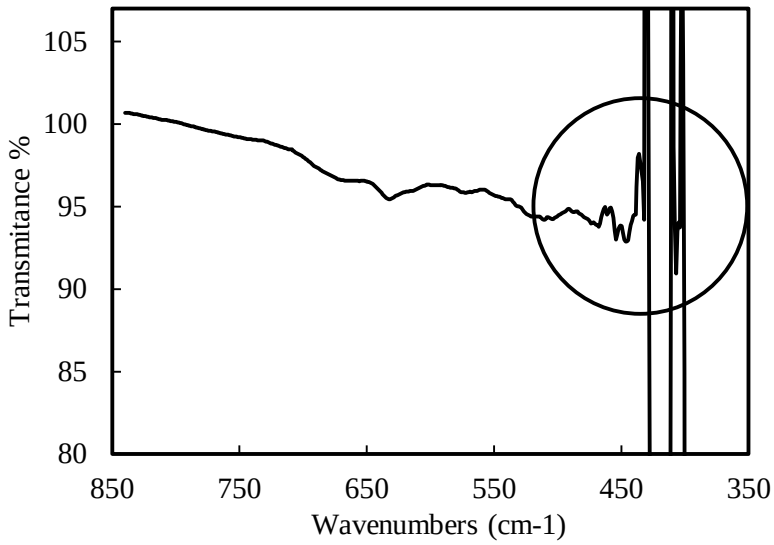

Figure 5-14 IM FTIR spectrum

Figure 5-14 presents the IR spectrum of the spent catalyst of the run conducted with the iron nitrate and molybdenum heptamolybdate precursors. The presence of peaks in the wavenumbers between 350 and 450 cm^{-1} shows that the precursors have been sulfurized to their active sulfide phase.

5.2 Hydrocracking of LVGO using (Dual catalyst system)

5.2.1 Catalytic activity on (Dual catalyst system)

Hydrocracking of LVGO using a dual catalyst system of Ni-LTM oleate complex precursor for the dispersed catalyst and a solid commercial catalyst (SC). The solid commercial catalyst consisted of silica alumina as support and tungsten with nickel as the active phase. This experiment was conducted to see the effect the dispersed catalyst will have on the solid catalyst.

The experiment was carried out with 30 g of LVGO as the feed, 3 g of solid catalyst and 0.0075 g of the dispersed oil soluble precursor. The experiment was conducted at temperatures of 400 °C, 415 °C and 430 °C and residence times of 15, 30, 45 and 60 minutes.

One run was conducted with the solid catalyst only (SC) at initial hydrogen pressure of 3.14 Mpa and initial temperature of 21.8 °C, the reaction temperature of 430 °C was reached after 74 minutes and residence time was 60 minutes. This run was conducted as control to compare the results of the following section.

The dispersed Ni-LTM oleate complex precursor and the solid catalyst (SC-LTM) were together added in the reactor with the feed. The reactor initial hydrogen pressure was 4.15 Mpa and the initial temperature was 25.5 °C, the reactor reached the reaction temperature of 430 °C after 71 minutes and the residence time was 60 minutes.

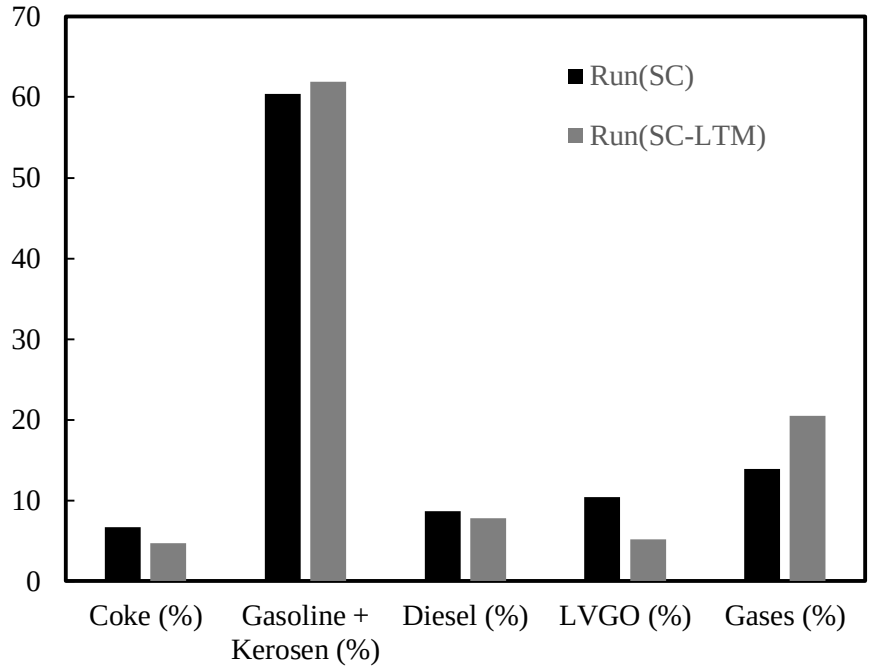

Figure 5-15 Product yield for Run(SC) and Run(SC-LTM)

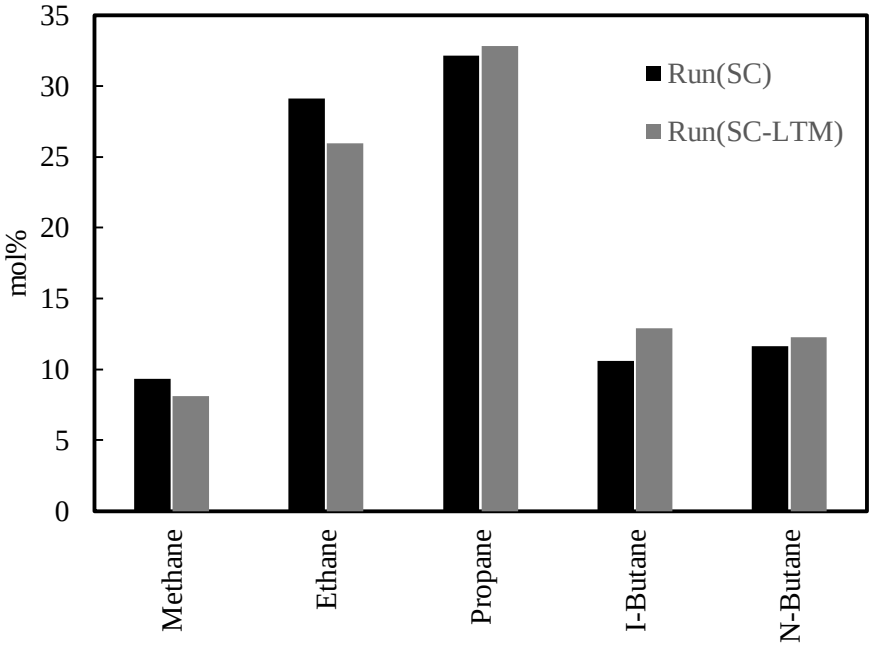

Figure 5-16 Gas distribution for Run(SC) and Run(SC-LTM)

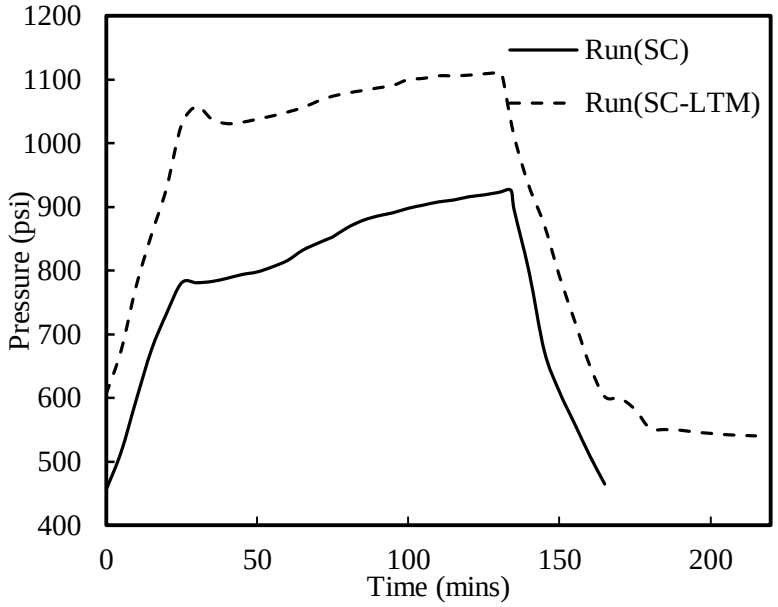

Figure 5-17 Pressure profiles for Run(SC) and Run(SC-LTM)

Different product yield of the run (SC) and run (SC-LTM) are represented in Figure 5-15, gas distribution for run (SC) and run (SC-LTM) are represented in Figure 5-16 and pressure profiles are represented in Figure 5-17.

The conversion for run (SC) is 73.84 % whereas, the conversion of run (SC-LTM) was 86.99 %. Comparing the product yield from Figure 5-15, the addition of Ni-LTM oleate complex precursor caused a decreases in the coke formed on the catalyst from 6.86 wt% in the run (SC) to 4.68 wt% in the run (SC-LTM), the coke formed per gram of catalyst decreased from 0.65 to 0.56 and the liquid yield was similar. However, the gas production was higher. Comparing the gas product distribution from Figure 5-16, the addition of Ni-LTM oleate complex precursor caused a decreases in all the gases expect propane.

From Figure 5-17 the initial and final hydrogen pressures for run (SC) are 456 psi and 429 psi whereas, the initial and final hydrogen pressures for run (SC-LTM) are 606 psi and

541 psi therefore, it can be shown that the addition of Ni-LTM oleate complex precursor caused a significant increase in the hydrogen consumption which is reflected in the lower coke formation for run (SC-LTM). The increase in the hydrogen consumption lead to the increase hydrogenation of the molecules leading to coke formation.

High molecular weight molecules undergo cracking either thermally or on the acid sites of the solid catalyst. These cracked molecules are not completely hydrogenated by the solid catalyst and react together to form coke on the solid catalyst surface. This cause the blocking of the active sites and which leads to catalyst deactivation. The presence of dispersed active phases cause an increase in the hydrogenation of these coke precursor molecules which leads to lower coke production.

Effect of reaction temperature

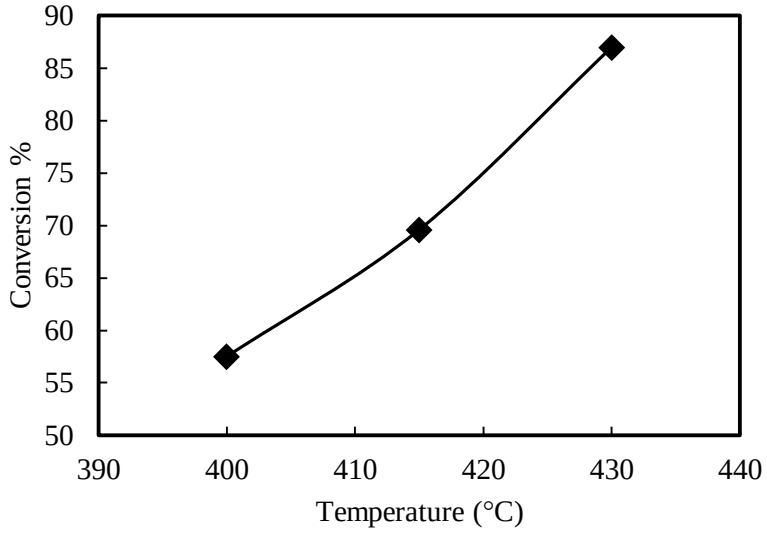

Figure 5-18 Conversion of (SC-LTM) at different temperatures

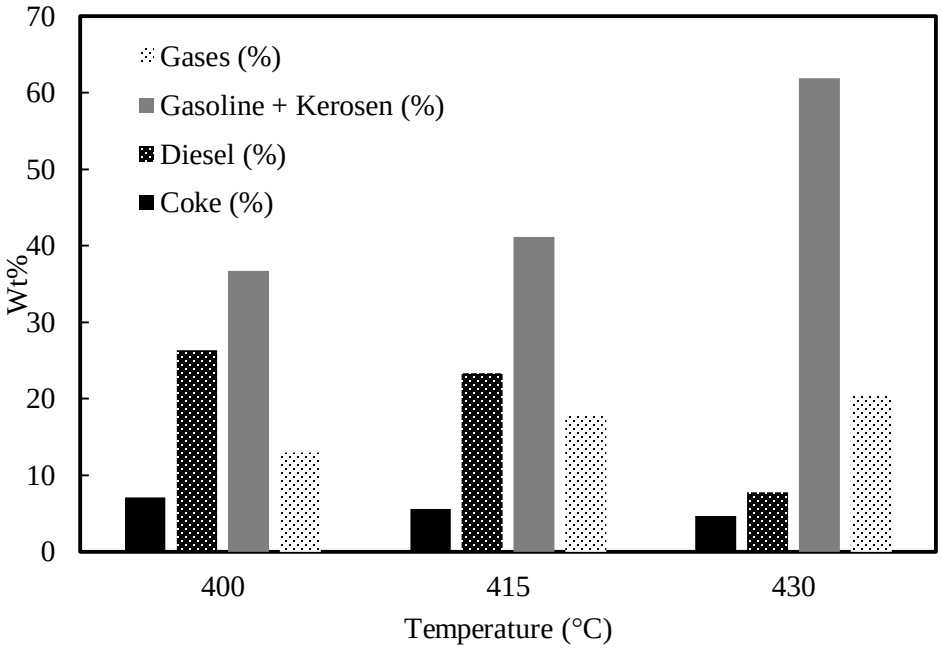

Figure 5-19 Product yield of (SC-LTM) at different temperatures

The product yield for (SC-LTM) at different temperatures are presented in Figure 5-19 and the conversion at different temperatures are presented in Figure 5-18. From Figure 5-18 it can be shown that as the temperature increases the conversion increases, the conversion increased from 67.00% at T=400 ℃ to 82.83% at T=430 ℃. From Figure 5-19 it can be shown that as the temperature increases the yield of the gasoline and kerosene fraction and the gases increases. Whereas, as the temperature increases the coke and diesel fraction decrease. Large asphaltic molecules especially the aromatic constituents of the asphaltenes need large amount of energy to break up the c-c bonds these are saturated in the presence high pressure hydrogen due to this fact as the temperature increases more and more of these asphaltic molecules break and are immediately saturated with hydrogen resulting in better products like gasoline and kerosene. This process limits the chance for coke to be formed from this asphaltic molecules.

Effect of residence time

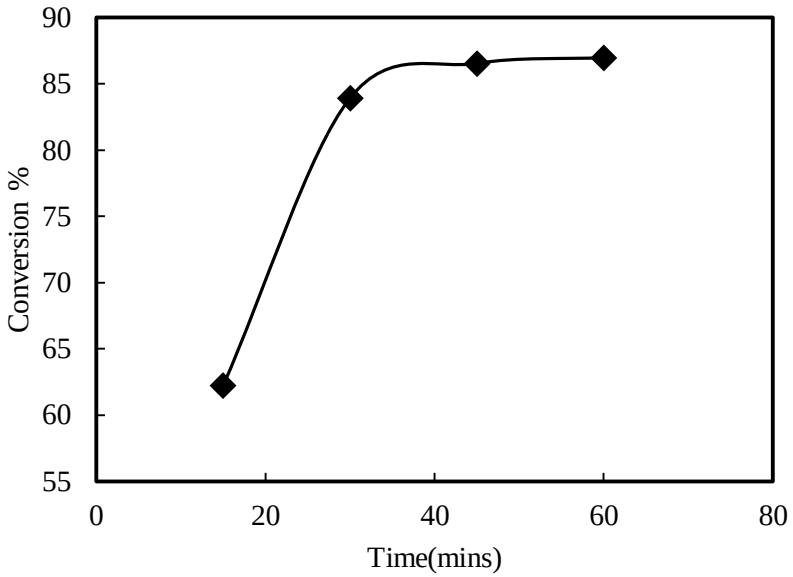

Figure 5-20 Conversion of (SC-LTM) at different residence times

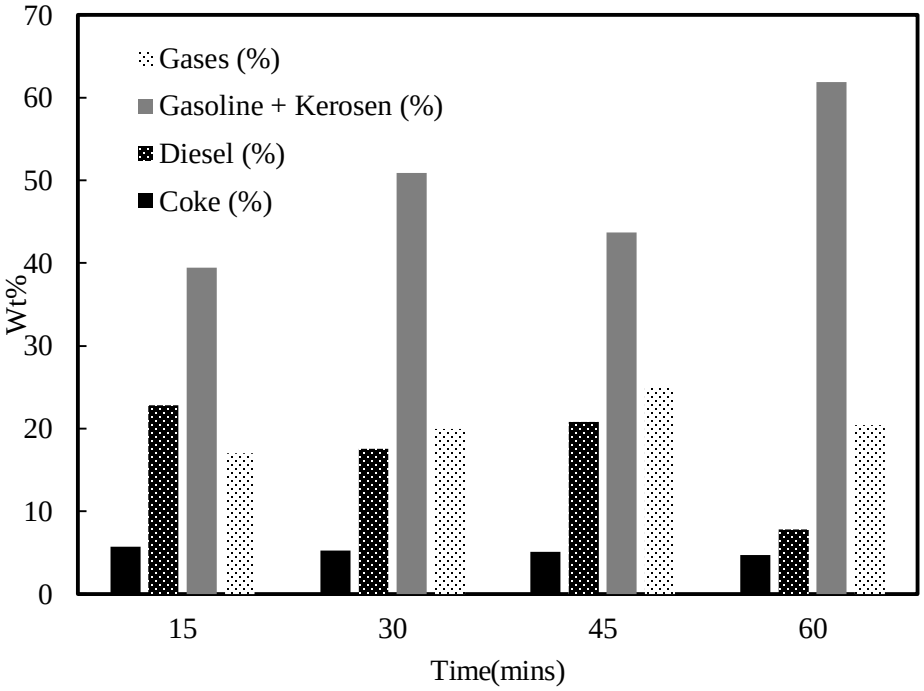

Figure 5-21 Product yield of (SC-LTM) at different times

The product yield for (SC-LTM) at different residence times are presented in Figure 5-21 and the conversion at different times are presented in Figure 5-20. From Figure 5-20 it can be shown that as the residence time increases the conversion increases, the conversion increased from 62.23% at t=15 mins to 86.56% at t=45 mins and increased to 86.99% at t=60 mins. As the residence time increases the gas production increases whereas, the gasoline and kerosene fraction start to increase from 39.42 wt% at t=15 mins to 50.90 wt% at t=30 mins and then decreases again to 43.69 wt% at t=45 mins and then increases again to 61.91 wt% at t=60 mins, similar patterns are observed for the other fractions. It can be concluded that temperature and the catalyst type have the major role in the selectivity of the products.

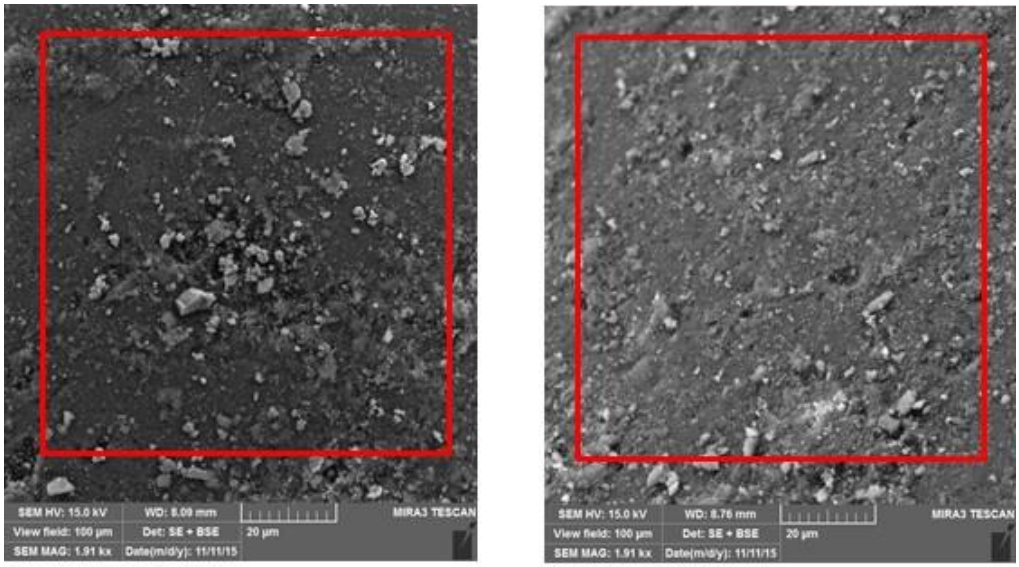

Figure 5-22 Spent catalyst SEM images

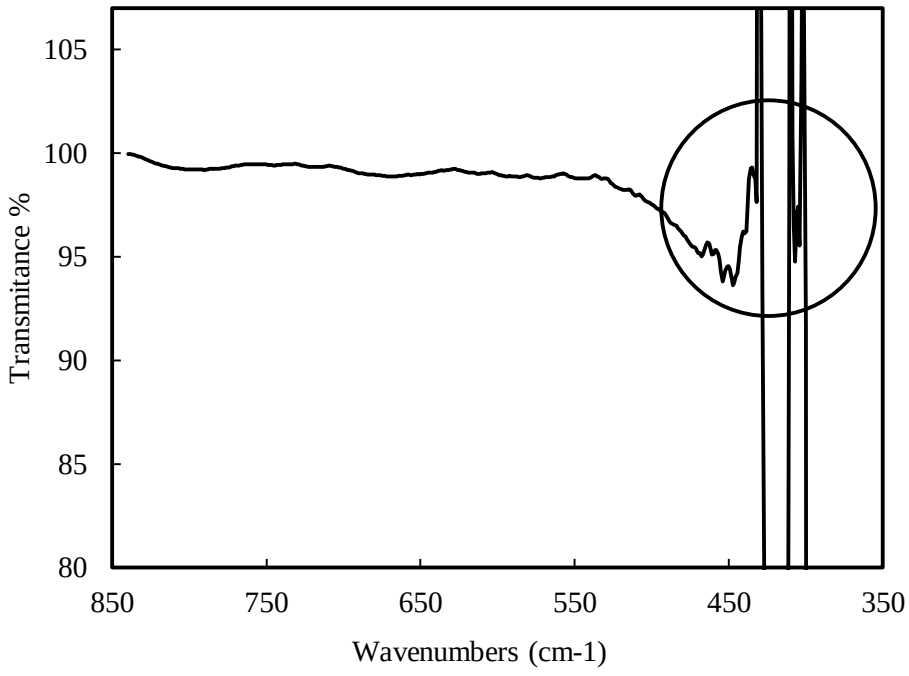

Figure 5-23 S.C + Ni-LTM FTIR spectrum

5.2.2 Characterization of the solid spent catalyst.

Figure 5-22 presents the SEM images of the spent catalyst of the S.C run and the S.C + Ni-LTM run, from this figure it can be shown that adding the oil soluble precursor caused a decrease in the number of active sites that are covered with coke.

Furthermore, Figure 5-23 presents the IR spectrum of the spent catalyst for the run conducted with the solid catalyst and Ni-LTM precursors. The presence of peaks in the wavenumbers between 350 and 450 cm^{-1} shows that the precursors have been sulfurized to their active sulfide phase.

CHAPTER 6

(H.C) Kinetics

6.1 Kinetic modelling of hydrocracking of VGO

6.1.1 Reaction scheme

There are many different products from different distillation cuts and chemical families for the catalytic cracking of VGO and therefore there are a great number of reaction possibilities with different mechanisms and steps involved [20], [21]. The lumping strategy has been always an effective way to simplify rate constants that are involved in the catalytic hydrocrackig of VGO, a 5- lump kinetic model is suitable representative of VGO hydrocracking kinetics [22], which is proposed by the following reaction scheme:

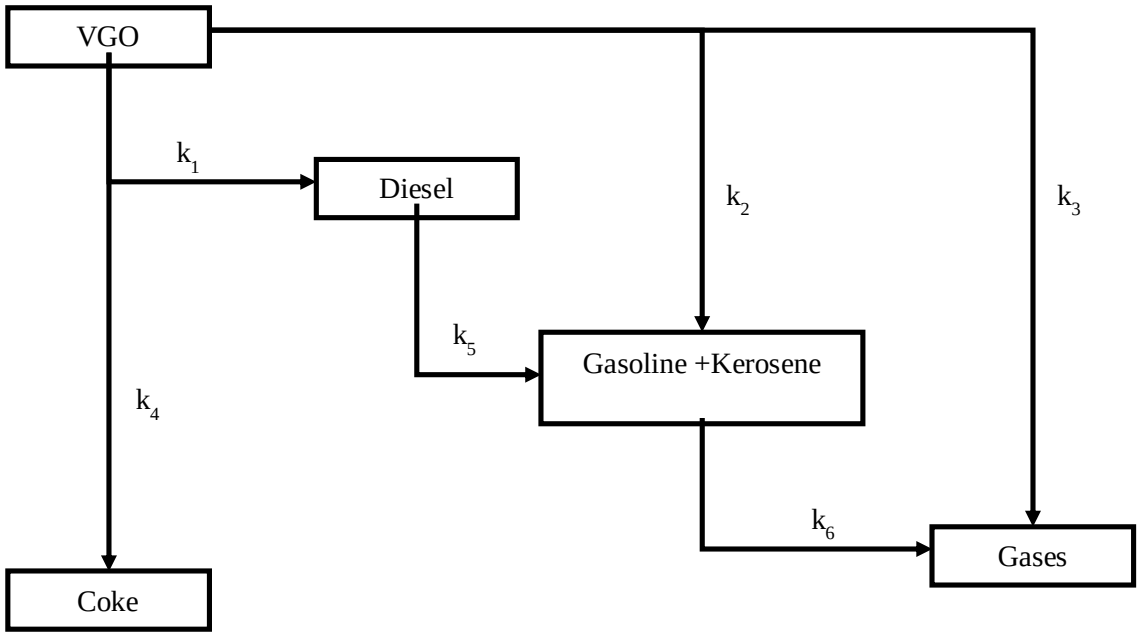

This model accounts for the cracking of VGO to diesel, gasoline and kerosene, gases and coke; the overcracking of diesel to gasoline and kerosene and the overcracking of

gasoline to gases. Previous studies found that the kinetic constants for the cracking reactions of diesel to coke; gasoline to coke and gases to coke were many orders of magnitudes smaller than the others [23], [24]. Taking this into account, we assumed that the formation of coke is only from the reaction of VGO lump.

Based on this proposed scheme, the equations gorverning VGO cracking, diesel, gasoline and kerosene, gas and coke formation are:

$$dM_{VGO} / dt = (- k_1 - k_2 - k_3 - k_4) (Y_{VGO})^2 \varphi W \quad \textbf{(6-1)}$$

$$dY_{Diesel} / dt = (k_1 (Y_{VGO})^2 - k_5 Y_{Diesel}) \varphi W \quad \textbf{(6-2)}$$

$$dY_{Gasoline} / dt = (k_2 (Y_{VGO})^2 - k_5 Y_{Diesel} - k_6 Y_{Gasoline}) \varphi W \quad \textbf{(6-3)}$$

$$dY_{Coke} / dt = k_4 (Y_{VGO})^2 \varphi W \quad \textbf{(6-4)}$$

$$dY_{Gas} / dt = (k_3 (Y_{VGO})^2 + k_6 Y_{Gasoline}) \varphi W \quad \textbf{(6-5)}$$

$$\varphi = \exp (-\alpha t) \quad \textbf{(6-6)}$$

Where φ is the deactivation function and W is the catalyst weight used. Furthermore, it is important to note that hydrogen is in excess which makes it possible to replace the hydrogen weight percentage by 1 making the equations simpler.

The model equations were formulated under the assumption that the cracking of VGO is second-order reaction, while all other reactions are first-order reaction. This is a widely adopted assumption in the literature based on the fact that VGO molecules are with changing reactivity[25].

A catalyst decay function φ is incorporated in the rate equations to account for the loss in catalyst activity due to deactivation from cocking. Exponential decay function which depends on residence time (t) is used to represent the catalyst decay term φ, as given in Eq. (6-1).

k_i are temperature dependent rate constants given by Arrhenius formula:

$$k_i = A_i \exp \left[\frac{-E_i}{RT} \right] \quad \textbf{(6-7)}$$

6.1.2 Determination of model parameters

The parameters of the five deferential equations incorporated with deactivation function were evaluated by the least-squares fitting of the experimental data. Data points were collected at 15, 30, 45 and 60 mins at three different temperatures of 400, 415 and 430 ^{o}C. The differential equations were solved using Runge-Kutta method (Mathematica's ParametricNdsolve) and for the parameter estimation the Levenberg-Marquardt algorithm (Mathematica's NonLinearModelFit) was used. The criteria used for optimization is that all the estimated parameters are positive.

The values of the estimated rate constants for the reactions [(6-1) to (6-5)] and the deactivation function at 400, 415, and 430 ^{o}C are listed in Table 6-1.

Table 6-1 Estimated rate constant

Reaction	Parameter	T = 400 °C	T = 415 °C	T = 430 °C
VGO → Diesel	k_1 ($kg_t\, kg_{vgo}^{-1}\, kg_{cat}^{-1}\, hr^{-1}$) × 100	1.72E-05	9.94E-06	1.08E-04
VGO → Gasoline + Kerosene	k_2 ($kg_t\, kg_{vgo}^{-1}\, kg_{cat}^{-1}\, hr^{-1}$) × 100	3.44E-04	9.14E-05	2.17E-03
VGO → Gases	k_3 ($kg_t\, kg_{vgo}^{-1}\, kg_{cat}^{-1}\, hr^{-1}$) × 100	31.83	22.50	40.91
VGO → Coke	k_4 ($kg_t\, kg_{vgo}^{-1}\, kg_{cat}^{-1}\, hr^{-1}$) × 100	40.93	42.77	57.47
Diesel → Gasoline + Kerosene	k_5 ($kg_{cat}^{-1}\, hr^{-1}$) × 100	141.28	344.12	416.35
Gasoline + Kerosene → Gases	k_6 ($kg_{cat}^{-1}\, hr^{-1}$) × 100	3.10E-07	121.34	7.76E-07
Deactivation	Φ (hr^{-1})	4.59	3.10	0.16

- kg_t is the total weight of the liquid product mixture
- kg_{vgo} is the weight of the VGO fraction in the liquid product mixture
- kg_{cat} is the catalyst weight

The Arrhenius plots for the hydrocracking of VGO to diesel, gasoline and kerosene, coke and gases are shown in Figure 6-1.

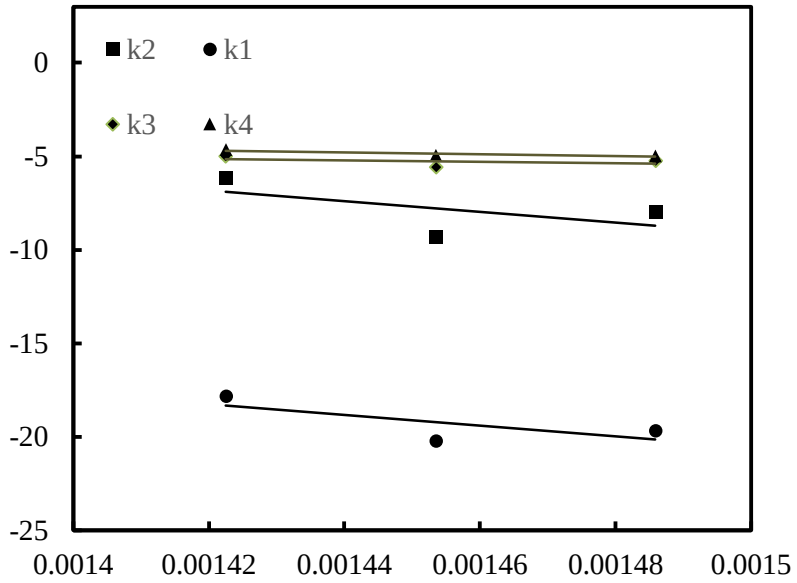

Figure 6-1 Arrhenius plot for H.C. of VGO

Table 6-2 Estimated activation energies

Product	k_i	E (kcal/mol)
VGO → Diesel	k_1	56.94
VGO → Gasoline + Kerosene	k_2	56.69
VGO → Gases	k_3	7.65
VGO → Coke	k_4	50.25
Diesel → Gasoline + Kerosene	k_5	34.03
Gasoline + Kerosene → Gases	k_6	37.52

Activation energies are reported in Table 6-2 the activation energies for the formation of diesel and the formation of the gasoline + kerosene cut are similar however comparing the rate constants for the conversion of VGO to diesel and the conversion of VGO to gasoline + kerosene cut it can be shown that it is more favorable for VGO to be converted to gasoline + kerosene. Furthermore, when comparing the activation energies for the formation of gases from VGO and the formation of gases from gasoline + kerosene, it can be shown that gases are most probably from the cracking of VGO rather than the cracking of gasoline + kerosene.

Comparing the activation energies for the formation of the gasoline + kerosene cut production form diesel and from VGO, it can be shown that it is more favorable for diesel to be cracked to gasoline + kerosene than VGO. Furthermore, the activation energy for the formation of coke from VGO is slightly less than the formation of diesel and the gasoline + kerosene cut from VGO which implies that the formation of coke is slightly more favorable than diesel and gasoline + kerosene.

CHAPTER 7

(HDS) Kinetics

7.1 Kinetics of the simultaneous HDS of model compounds

7.1.1 Introduction

A number of CoMo/γ-Al_2O_3 catalysts modified with P_2O_5 were prepared. The phosphorus concentration varied from 0.0 to 1.0 wt.% P_2O_5. All the catalysts prepared were evaluated in a batch autoclave reactor to investigate the effect of P_2O_5 on the simultaneous hydrodesulfurization (HDS) of dibenzothiophene (DBT) and 4-methyl dibenzothiophene (4-MDBT). The HDS expriments were conducted using 500 ppm DBT and 500 ppm 4-MDBT and with diffrenets temperatures levels. The product analysis show that the products of the HDS of DBT are biphenyl (BP) via the direct desulfurization route (DDS) and cyclohexyl benzene (CHB) via the hydrogenation route (HYD), similarly the products from the HDS of 4-MDBT are methyl biphenyl (MBP) via the DDS route and 3-methyl-1-cyclohexylbenzene (MCHB) via the HYD route. The Langmuir-Hinshelwood mechanism is proposed for the simultaneous HDS of DBT and 4-MDBT. The analysis of the proposed model suggests that the catalyst used are more selective to the HDS of DBT than the HDS of 4-MDBT, furthermore the addition of P_2O_5 favored the DDS pathway over the HYD pathway for both DBT and 4-MDBT.

7.1.2 HDS of DBT and 4-MDBT

The distribution of the products resulting from the HDS of DBT and 4-MDBT at 350°C over CMP(0) and CMP(1) catalysts are presented in Figure 7-1. It can be observed that

HDS of DBT and 4-MDBT proceeded predominantly via DDS pathway and 1wt.% P_2O_5 enhanced the HDS via both pathways. However, the enhancement on DDS pathway was significantly higher for HDS of 4-MDBT than DBT [26].

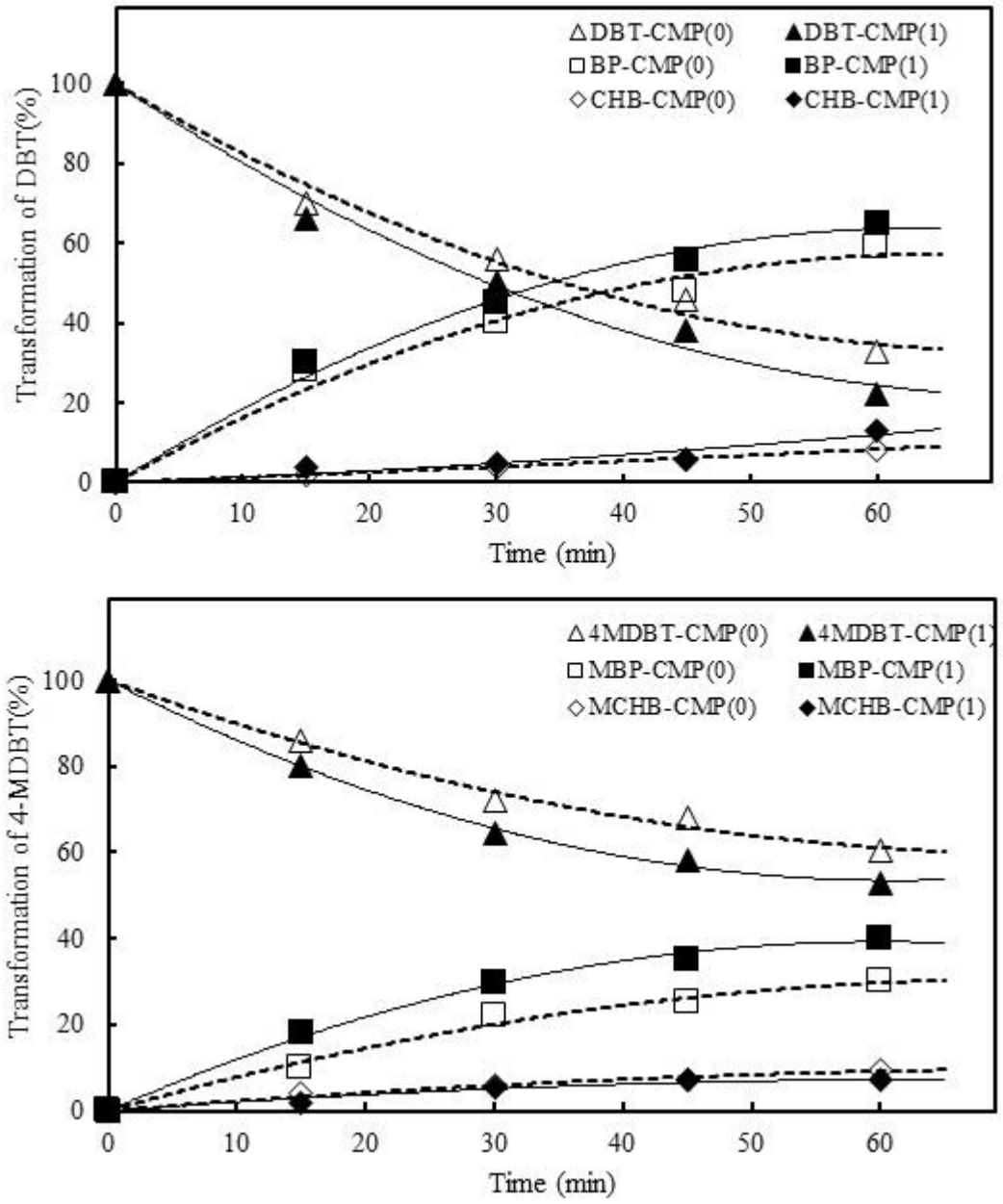

Figure 7-1 Product distribution during simultaneous HDS of DBT [A] and 4-MDBT [B] over CMP(0) and CMP(1) catalysts at 623 K.

7.1.3 Mechanism of HDS and its Pathways

The HDS of DBT and 4-MDBT occurs via two routes: DDS or HYD. DDS is the direct desulfurization or hydrogenolysis by C-S bond scission while the HYD involves hydrogenation of one the phenyl rings prior to C-S bond scission [27]. HDS of DBT by DDS produces biphenyl (BP) and H_2S while the HYD pathway yields transitional compounds like tetrahydro dibenzothiophene (THDBT) and hexahydro dibenzothiophene (HHDBT) which are quickly desulfurized to cyclohexyl benzene (CHB). Similarly, HDS of 4-MDBT by DDS produces methyl biphenyl (MBP) and HDS by HYD produces 3-methyl-1-cyclohexybenzene (MCHB) as the partial hydrogenated hydrocarbon product.

Figure 7-2 (A) and Figure 7-2 (B) show a simple scheme for the reaction pathways of the DBT and 4-MDBT, respectively. DDS consumes less hydrogen therefore it is the preferred pathway. The intermediates produced during the HDS of DBT and 4-MDBT through the HYD pathway were found to be very low in concentrations and the major products produced from the HYD pathway were CHB and MCHB. Taking into account what preceded, the flowing reaction scheme is suggested for the kinetic modeling:

$$\boldsymbol{DBT + H_2 \xrightarrow{k_1} BP + H_2S} \quad \textbf{(7-1)}$$

$$\boldsymbol{DBT + H_2 \xrightarrow{k_2} CHB + H_2S} \quad \textbf{(7-2)}$$

$$\boldsymbol{4MDBT + H_2 \xrightarrow{k_3} MBP + H_2S} \quad \textbf{(7-3)}$$

$$\boldsymbol{4MDBT + H_2 \xrightarrow{k_4} MCHB + H_2S} \quad \textbf{(7-4)}$$

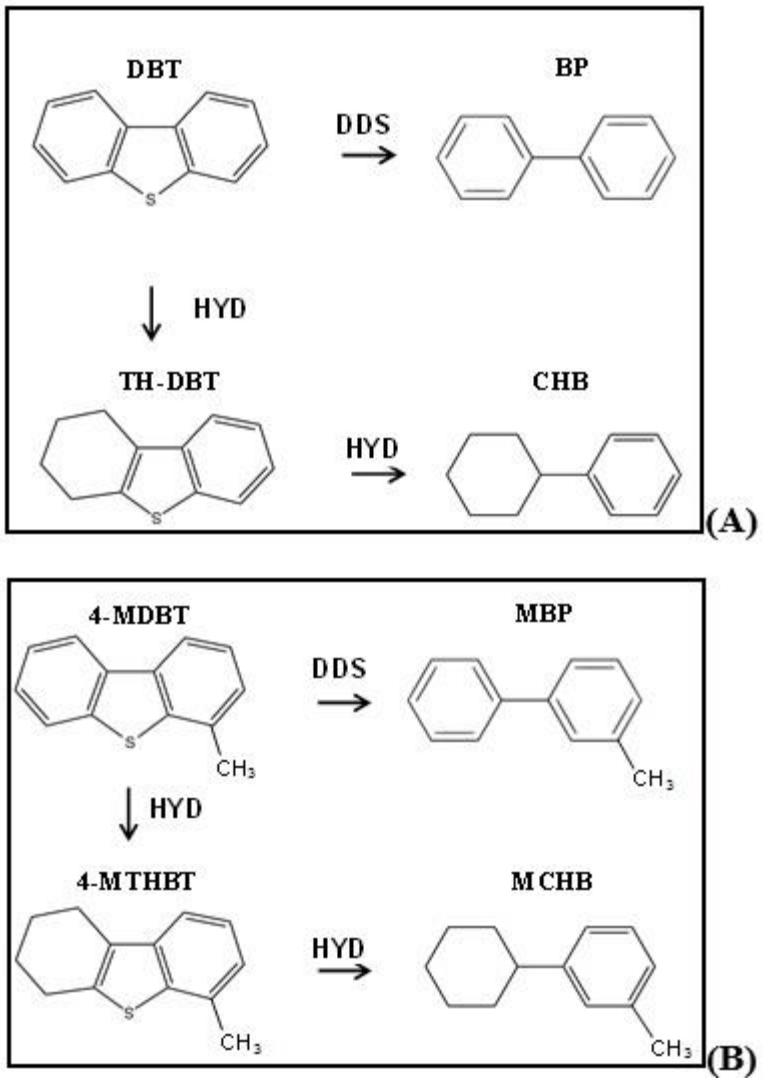

Figure 7-2 Reaction pathways Scheme for (A) DBT and (B) 4-MDBT.

7.1.4 Development of Kinetic Model for the Simultaneous HDS of DBT and 4-MDBT

On the basis of above discussion, a kinetic model for simultaneous HDS of DBT and 4-MDBT is proposed which include surface reactions controlled by Langmuir-Hinshelwood mechanism. The steps involved in the overall reaction mechanism are as follows:

(i) Adsorption of DBT:

$$DBT_{(g)} + X \leftrightarrow DBT - X \quad \textbf{(7-5)}$$

(ii) Adsorption of hydrogen:

$$H_{2(g)} + X \leftrightarrow H_2 - X \quad \textbf{(7-6)}$$

(iii) Adsorption of 4-MDBT:

$$4MDBT_{(g)} + X \leftrightarrow 4MDBT - X \quad \textbf{(7-7)}$$

(iv) Surface reactions:

$$DBT - X + H_2 - X \rightarrow BP - X + H_2S_{(g)} \quad \textbf{(7-8)}$$

$$DBT - X + H_2 - X \rightarrow CHB - X + H_2S_{(g)} \quad \textbf{(7-9)}$$

$$4MDBT - X + H_2 - X \rightarrow MBP - X + H_2S_{(g)} \quad \textbf{(7-10)}$$

$$4MDBT - X + H_2 - X \rightarrow MCHB - X + H_2S_{(g)} \quad \textbf{(7-11)}$$

(v) Desorption of products:

$$BP - X \leftrightarrow BP_{(g)} + X \quad \textbf{(7-12)}$$

$$CHB - X \leftrightarrow CHB_{(g)} + X \quad \textbf{(7-13)}$$

$$MBP - X \leftrightarrow MBP_{(g)} + X \quad \textbf{(7-14)}$$

$$MCHB - X \leftrightarrow MCHB_{(g)} + X \quad \textbf{(7-15)}$$

The reaction rates for the surface reactions [(7-15) to (7-18)] are as follows:

$$r_1 = k_1\theta_{DBT}\,\theta_{H_2} \quad \textbf{(7-16)}$$

$$r_2 = k_2\theta_{DBT}\,\theta_{H_2} \quad \textbf{(7-17)}$$

$$r_3 = k_3\theta_{4MDBT}\,\theta_{H_2} \quad \textbf{(7-18)}$$

$$r_4 = k_4\theta_{4MDBT}\,\theta_{H_2} \quad \textbf{(7-19)}$$

The fractional coverage for DBT, MDBT and H_2 are expressed as:

$$\theta_{DBT} = \frac{C_{DBT}}{(1+K_{DBT}C_{DBT}+K_{4MDBT}C_{4MDBT})} \quad \textbf{(7-20)}$$

$$\theta_{H_2} = \frac{1}{(1+K_{DBT}C_{DBT}+K_{4MDBT}C_{4MDBT})} \quad \textbf{(7-21)}$$

$$\theta_{4MDBT} = \frac{C_{4MDBT}}{(1+K_{DBT}C_{DBT}+K_{4MDBT}C_{4MDBT})} \quad \textbf{(7-22)}$$

It is important to note that hydrogen is in excess which makes it possible to have one as the numerator of the fractional coverage for hydrogen. Furthermore, the adsorption constant of hydrogen is negligible.

The relation between the reaction rates and the concentration of the involving species is described by the mole balance of the reactants and the products species during the HDS of DBT and 4-MDBT in the batch reactor.

The mole balance was governed by certain assumptions and they are as follows:

i. The HDS reactions are irreversible.

ii. Thermal cracking of the model compounds is neglected. This assumption was confirmed by conducting experimental runs in the absence of the catalyst.

iii. Isothermal conditions are assumed which is confirmed by negligible temperature fluctuation observed during the reaction runs.

Considering the above assumptions, the following set of differential equations describes the mole balance of the various species present in the reaction medium.

(i) Rate of formation of BP

$$\frac{dC_{BP}}{dt} = r_1 \qquad \textbf{(7-23)}$$

(ii) Rate of formation of CHB

$$\frac{dC_{CHB}}{dt} = r_2 \qquad \textbf{(7-24)}$$

(iii) Rate of disappearance of DBT

$$-\frac{dC_{DBT}}{dt} = r_1 + r_2 \qquad \textbf{(7-25)}$$

(iv) Rate of formation of MBP

$$\frac{dC_{MBP}}{dt} = r_3 \quad \textbf{(7-26)}$$

(v) Rate of formation of MCHB

$$\frac{dC_{MCHB}}{dt} = r_4 \quad \textbf{(7-27)}$$

(vi) Rate of disappearance of 4-M DBT

$$-\frac{dC_{4MDBT}}{dt} = r_3 + r_4 \quad \textbf{(7-28)}$$

where C_i is the molar concentration of species *i* at any time *t*.

7.1.5 Parameter Estimation and Model Discrimination

The parameters of the mole balance equations incorporated with the Langmuir Hinshelwood models were evaluated by the least-squares fitting of the experimental data for the HDS of DBT with 4-MDBT. Data points were collected at 15, 30, 45 and 60 mins at three different temperatures of 300, 325 and 350 ^{o}C. The differential equations were solved using Runge-Kutta method (Mathematica's ParametricNdsolve) and for the parameter estimation the Levenberg-Marquardt algorithm (Mathematica's NonLinearModelFit) was used. The criteria used for optimization is that all the estimated parameters are positive.

Coefffient of determination (R^2), lowest sum of squares of the residuals (SSR), cross correlation matrix and minimum individual confidence intervals were used for the model discrimination of the estimated parameters. The cross correlation matrix for CMP(0) at T=350°C is shown below:

$$\begin{pmatrix} * & k_1 & k_2 & k_3 & k_4 & K_1 & K_2 \\ k_1 & 1 & 0.131 & 0.091 & 0.031 & 0.771 & 0.762 \\ k_2 & 0.131 & 1 & 0.030 & 0.010 & 0.261 & 0.262 \\ k_3 & 0.091 & 0.010 & 1 & -0.310 & 0.119 & 0.118 \\ k_4 & 0.031 & 0.010 & -0.310 & 1 & 0.041 & 0.040 \\ K_1 & 0.772 & 0.261 & 0.119 & 0.041 & 1 & 0.999 \\ K_2 & 0.762 & 0.262 & 0.118 & 0.040 & 0.999 & 1 \end{pmatrix} \quad \textbf{(7-29)}$$

The values of the estimated rate constants for the surface reactions [(6-15) to (6-18)] using catalysts CMP(0), CMP(0.5) and CMP(1) at 300, 325, and 350 ^{o}C are listed in Table 7-1. The rate constant for the formation of BP is always higher than the rate constant for the formation of CHB. Similarly the rate constant for the formation of MBP is always higher than the rate constant of MCHB. These observations indicate that the HDS of the model compounds through the DDS route is faster than the HDS through the HYD route. Futhermore, the rate constant for the formation of BP and CHB is always higher than the respective rate constant for the formation of MBP and MCHB. These results indicate that the catalysts used in this study are more selective towards DBT than 4-MDBT.

Table 7-1 Estimated rate constants

Catalyst				CMP(0)		CMP(0.5)		CMP(1)	
Temperature (ºC)	**Sulfur Compound**	**HDS Route**		***k* × 100 (min^{-1})**	**Confidence Interval**	***k* × 100 (min^{-1})**	**Confidence Interval**	***k* × 100 ($min^{-1)}$**	**Confidence Interval**
300	DBT	DDS	k_1	0.30	{0.202, 0.394}	0.35	{0.304, 0.397}	0.32	{0.204, 0.429}
	DBT	HYD	k_2	0.04	{0.006, 0.070}	0.06	{0.029, 0.096}	0.05	{0.015, 0.092}
	4MDBT	DDS	k_3	0.10	{0.05, 0.147}	0.14	{0.101, 0.178}	0.17	{0.100, 0.233}
	4MDBT	HYD	k_4	0.04	{0.004, 0.066}	0.04	{0.005, 0.068}	0.03	{0.000, 0.068}
310	DBT	DDS	k_1	0.38	{0.382, 0.388}	0.47	{0.350, 0.593}	0.40	{0.389, 0.412}
	DBT	HYD	k_2	0.04	{0.049, 0.050}	0.07	{0.055, 0.095}	0.07	{0.071,0.088}
	4MDBT	DDS	k_3	0.13	{0.138, 0.141}	0.20	{0.151, 0.264}	0.21	{0.204, 0.226}
	4MDBT	HYD	k_4	0.04	{0.045, 0.046}	0.04	{0.028, 0.052}	0.04	{0.035, 0.521}
325	DBT	DDS	k_1	0.49	{0.381, 0.606}	0.52	{0.334, 0.701}	0.59	{0.508, 0.675}
	DBT	HYD	k_2	0.06	{0.009, 0.119}	0.07	{0.011, 0.131}	0.08	{0.009, 0.160}
	4MDBT	DDS	k_3	0.20	{0.121, 0.272}	0.25	{0.163, 0.329}	0.30	{0.218, 0.379}
	4MDBT	HYD	k_4	0.06	{0.006, 0.112}	0.04	{0.000, 0.095}	0.05	{0.000, 0.122}
335	DBT	DDS	k_1	0.92	{0.926, 0.930}	1.02	{1.027, 1.030}	1.08	{1.043, 1.125}
	DBT	HYD	k_2	0.11	{0.115, 0.117}	0.14	{0.140, 0.141}	0.16	{0.154, 0.167}
	4MDBT	DDS	k_3	0.36	{0.365, 0.367}	0.45	{0.450, 0.453}	0.55	{0.528, 0.574}
	4MDBT	HYD	k_4	0.11	{0.114, 0.117}	0.09	{0.097, 0.098}	0.09	{0.091, 0.100}
350	DBT	DDS	k_1	1.71	{1.545, 1.878}	1.92	{1.719, 2.117}	2.08	{1.866, 2.286}
	DBT	HYD	k_2	0.22	{0.133, 0.299}	0.25	{0.145, 0.347}	0.31	{0.208, 0.416}
	4MDBT	DDS	k_3	0.70	{0.630, 0.770}	0.82	{0.737, 0.904}	1.03	{0.942, 1.117}
	4MDBT	HYD	k_4	0.21	{0.150, 0.279}	0.19	{0.116, 0.268}	0.19	{0.112, 0.265}

The Arrhenius plot for the HDS of DBT by DDS route, shown in Figure 7-3, indicate that the influence of variation in catalyst composition on reaction rate was not significant. However, the Arrhenius plot for the HDS of 4-MDBT by DDS route, shown in , indicate that catalyst containing 1% phoshphorus [CPM(1)] exhibited higher reaction rate compared to phosphorus-free catalyst [CPM(0)].

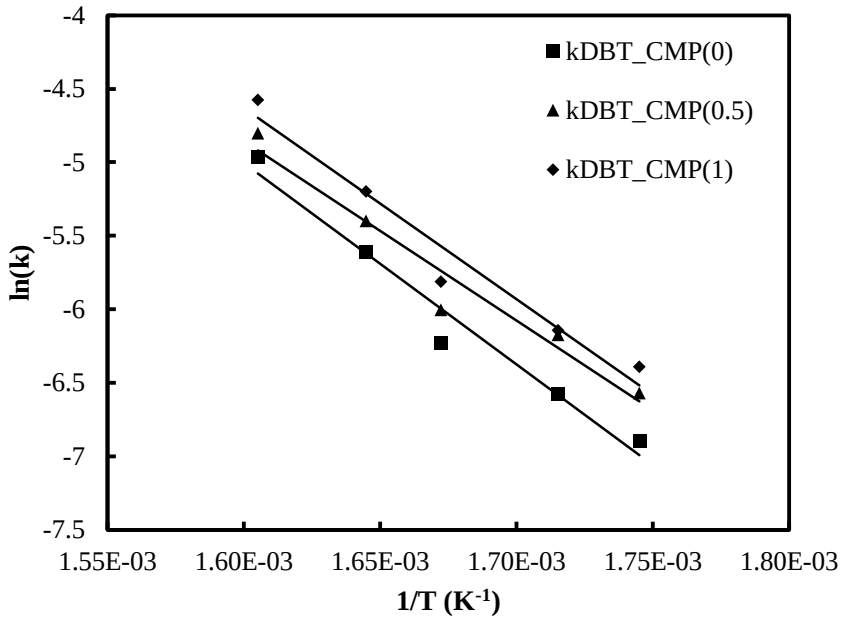

Figure 7-3 Arrhenius plot for HDS of DBT by DDS route

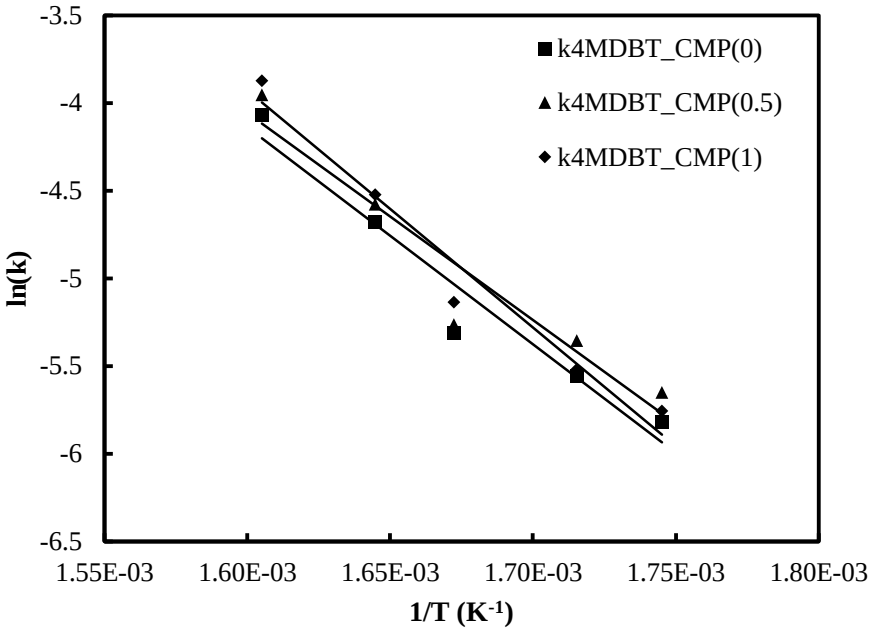

Figure 7-4 Arrhenius plot for HDS of 4-MDBT by DDS route.

The estimated adsorption equilibrium constants for the model are listed in Table 7-2. The mathimatica code failed to estimate these parameters with reasonable low confidence interval. However the adsorption constants follow the Van't Hoff equation as presented in the Van't Hoff plots for the HDS of DBT in Figure 7-5 and for the HDS of 4MDBT in Figure 7-6. From Table 7-2 it can be noticed that the adsorption equilibrium for DBT is higher than the adsorption of 4-MDBT which indicate that the catalysts CMP(0), CMP(0.5) and CMP(1) are more selective for HDS of DBT than HDS of 4-MDBT.

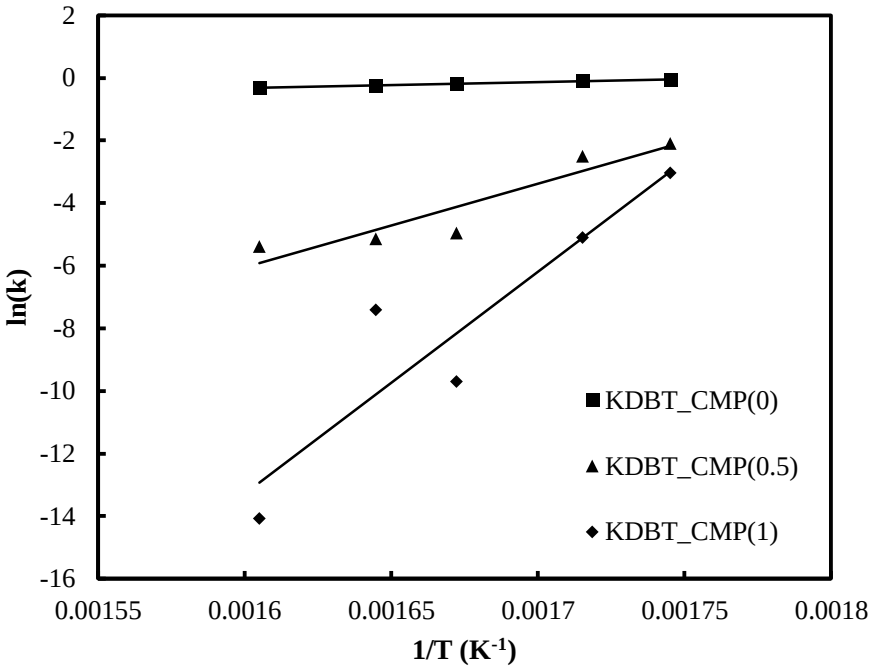

Figure 7-5 Van't Hoff plot for HDS of DBT.

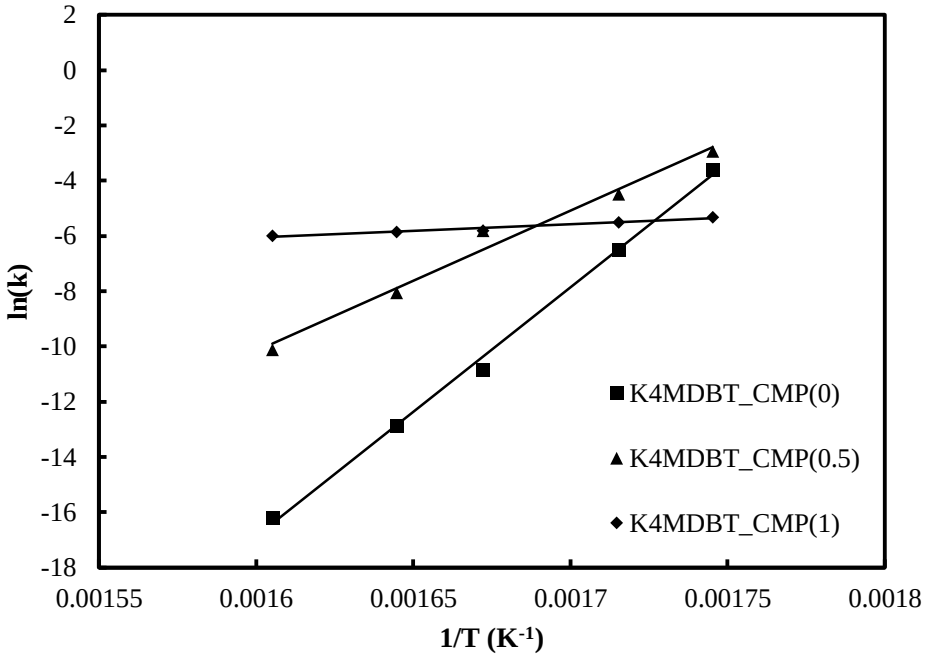

Figure 7-6 Van't Hoff plot for HDS of 4-MDBT

Table 7-2 Estimated equlibrium adsorption constants.

Catalyst		CMP(0)		CMP(0.5)		CMP(1)	
		K **(l/mol)**	**Confidence Interval**	***K*** **(l/mol)**	**Confidence Interval**	***K*** **(l/mol)**	**Confidence Interval**
300 ºC	K_1	0.9458569	High	0.1245920	High	0.0485317	High
	K_2	0.0281252	High	0.0531081	High	0.0048798	High
310 ºC	K_1	0.91231424	High	0.0822138	High	0.0061654	High
	K_2	0.0015212	High	0.0112470	High	0.0040654	High
325 ºC	K_1	0.8404890	High	0.0069998	High	0.0000610	High
	K_2	0.0000199	High	0.0030502	High	0.0030475	High
335 ºC	K_1	0.7816932	High	0.0059093	High	0.0006021	High
	K_2	0.0000026	High	0.0003160	High	0.0029001	High
350 ºC	K_1	0.7327390	High	0.0046256	High	0.0000008	High
	K_2	0.0000001	High	0.0000406	High	0.0025036	High

Activation energies are reported in Table 7-3. The values of the activation energy for the formation of BP when using the catalyst CMP(0) is 103 kJ/mol whereas the activation energy for the formation of CHB is slightly less at 102 kJ/mol. This observation shows that at low temperatures the catalyst is more selective towards the HYD route and at high temperatures the catalyst is more slelective towards the DDS route. Futhermore, the activation energy for the formation of BP when using the catalyst CMP(0.5) is 99 kJ/mol whereas it is 111 kJ/mol when using the catalyst CMP(1). Similarly the activation energy of formation of CHB for CMP(0.5) is 79 kJ/mol and for CMP(1) is 103 kJ/mol. This result shows that as the percentage of P2O5 increases the activity of the catalyst increases up to phosphorus content of 1 wt%. A similar trend is observed with MBP and MCHB.

Table 7-3 Estimated activation energies for HDS of DBT and 4-MDBT via DDS and HYD pathways

Activation Energy (kJ/mol)	CMP(0)	Confidence Interval	CMP(0.5)	Confidence Interval	CMP(1)	Confidence Interval
$\boldsymbol{E}_1$	103.0	{57.6,148.6}	98.1	{41.5,154.7}	112.4	{71.6,153.2}
$\boldsymbol{E}_2$	102.4	{58.8,145.3}	78.4	{12.4,144.5}	99.1	{43.9,154.3}
$\boldsymbol{E}_3$	114.0	{75.1,152.7}	101.4	{58.7,144}	108.0	{67.0,149.1}
$\boldsymbol{E}_4$	106.7	{59.7,154.5}	98.7	{22.1,175.4}	99.5	{48.6,150.4}

A comparison of the concentrations for DBT, BP, CHB, 4-MDBT, MBP and MCHB as predicted by the kinetic model and the experimentally determined concentrations at 350°C are presented as a parity plot on Figure 7-7. From the plot, it be observed that the predicted concentration by the kinetic model matches the experimental concentration in an excellent manner.

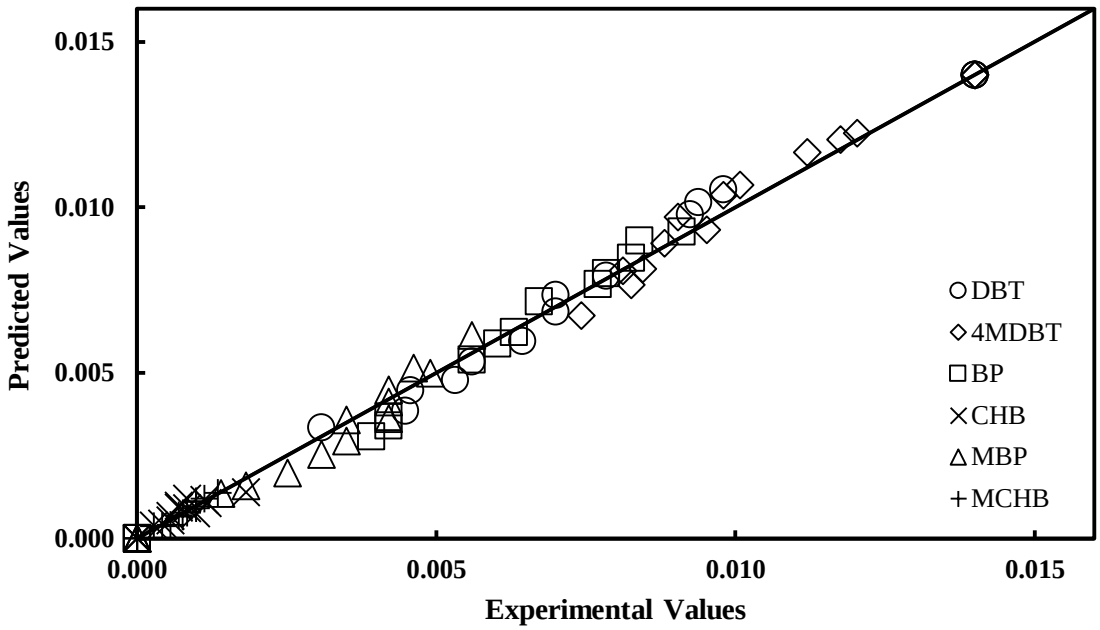

Figure 7-7 Parity plot between experimental values of product composition (wt%) and the values predicted by kinetic model.

CHAPTER 8

Conclusion and Recommendations

8.1 Conclusions

The following are the conclusions of the effects of dispersed catalysts on the heavy oil (VGO) upgrading:

- The presence of dispersed catalysts enhanced the hydrogen consumption indicating the improved hydrogenation activity.
- Mixtures of the dispersed catalyst decreased the coke formation significantly.
- A higher yield in gas products was observed with the water soluble bimetallic catalyst more than the oil soluble bimetallic catalyst.
- Water soluble bimetallic catalyst are selective towards hydrogenating coke precursors to gaseous products.
- A higher yield in liquid products is observed with oil soluble bimetallic catalysts than the water soluble bimetallic catalyst.
- Oil soluble bimetallic catalyst are selective towards hydrogenating coke precursors to liquid products.
- As temperature increased the coke production decreased because of the cumulative effect of the oil soluble bimetallic dispersed catalyst with the solid (H.C) catalyst increased.

- As temperature increased the cumulative hydrogenation effect of the oil soluble bimetallic dispersed catalyst with the solid (H.C) catalyst increased.

- It is more favorable for VGO to be converted to gasoline and kerosene than diesel.

- Diesel present in the VGO is more likely to be converted to gasoline and kerosene which increased the yield of Gasoline and kerosene fraction.

- Gases are more favorable to be produced from the cracking of VGO rather than cracking of (gasoline + kerosene) and diesel fractions.

- A five lumped kinetics model fitted the experimental data adequately.

- The specific reaction rate of gasoline and kerosene formation is significantly higher than that of diesel formation.

The following conclusions of HDS of model compounds using CoMo/P2O5-Al_2O_3 catalyst:

- Addition of P_2O_5 to CoMo/γ-Al_2O_3 catalyst increased the HDS activity.

- A comparison of the reaction rates constants for the formation of BP, CHB, MBP and MCHB and the activation energies show that the simultaneous HDS of DBT and 4-MDBT occur mostly by DDS route rather than HYD route – especially at high temperatures.

- By comparing the activation energies for the formation of BP, CHB, MBP and MCH and the equilibrium adsorption rate constants it can be concluded that CoMo/P-Al_2O_3 catalysts are more selective towards the HDS of DBT over the HDS of 4-MDBT.

8.2 Recommendations

- Extensive research could be done on a single model compound to better understand the kinetics of hydrocracking of heavy hydrocarbon liquids by the aid of dispersed catalyst.

- More research could be directed for the HDS and HDN reaction enhancement caused by adding the dispersed catalyst to the solid hydrocracking catalysts

Reference

[1] G. Bellussi, G. Rispoli, A. Landoni, R. Millini, D. Molinari, E. Montanari, D. Moscotti, and P. Pollesel, "Hydroconversion of heavy residues in slurry reactors: Developments and perspectives," *J. Catal.*, vol. 308, pp. 189–200, Dec. 2013.

[2] Y. Liu, L. Gao, L. Wen, and B. Zong, "Recent Advances in Heavy Oil Hydroprocessing Technologies," *Recent Patents Chem. Eng.*, vol. 2, no. 1, pp. 22–36, Jan. 2009.

[3] I. Chorkendorff and J. . Niemantverdriet, *Concepts of Modern Catalysis and Kinetics*. 2003.

[4] R. Bacaud, "Dispersed phase catalysis: Past and future. Celebrating one century of industrial development," *Fuel*, vol. 117, pp. 624–632, Jan. 2014.

[5] H. Ortiz-Moreno, J. Ramírez, R. Cuevas, G. Marroquín, and J. Ancheyta, "Heavy oil upgrading at moderate pressure using dispersed catalysts: Effects of temperature, pressure and catalytic precursor," *Fuel*, vol. 100, pp. 186–192, Oct. 2012.

[6] A. Jain and B. Pruden, "Hydrocraking of Heavy Oils in Presence of Petroleum Coke Derived from Heavy Oil Coking Operations," US4999328, 1991.

[7] C. P. Khulbe, R. Ranganathan, and B. B. Pruden, "Hydrocracking of heavy Oils/Fly Ash Slurries," US4299685, 1981.

[8] L. C. Castañeda, J. a. D. Muñoz, and J. Ancheyta, "Current situation of emerging technologies for upgrading of heavy oils," *Catal. Today*, vol. 220–222, pp. 248–273, Mar. 2014.

[9] Y. G. Hur, M.-S. Kim, D.-W. Lee, S. Kim, H.-J. Eom, G. Jeong, M.-H. No, N. S. Nho, and K.-Y. Lee, "Hydrocracking of vacuum residue into lighter fuel oils using nanosheet-structured WS2 catalyst," *Fuel*, vol. 137, pp. 237–244, Dec. 2014.

[10] H.-J. Eom, D.-W. Lee, S. Kim, S.-H. Chung, Y. G. Hur, and K.-Y. Lee, "Hydrocracking of extra-heavy oil using Cs-exchanged phosphotungstic acid (CsxH3−xPW12O40, x=1–3) catalysts," *Fuel*, vol. 126, pp. 263–270, Jun. 2014.

[11] G. Bellussi, G. Rispoli, D. Molinari, A. Landoni, P. Pollesel, N. Panariti, R. Millini, and E. Montanari, "The role of MoS2 nano-slabs in the protection of solid cracking catalysts for the total conversion of heavy oils to good quality distillates," *Catal. Sci. Technol.*, vol. 3, no. 1, p. 176, 2013.

[12] S. G. Jeon, J. G. Na, C. H. Ko, K. B. Lee, N. S. Rho, and S. Bin Park, "A new approach for preparation of oil-soluble bimetallic dispersed catalyst from layered ammonium nickel molybdate," *Mater. Sci. Eng. B Solid-State Mater. Adv. Technol.*, vol. 176, no. 7, pp. 606–610, Apr. 2011.

[13] H. Luo, W. Deng, J. Gao, W. Fan, and G. Que, "Dispersion of water-soluble

catalyst and its influence on the slurry-phase hydrocracking of residue," *Energy and Fuels*, vol. 25, no. 3, pp. 1161–1167, 2011.

[14] G. F. Froment, "The kinetics of complex catalytic reactions," *Chem. Eng. Sci.*, vol. 42, pp. 1073–1087, 1987.

[15] M. R. Gray, "Lumped kinetics of structural groups: hydrotreating of heavy distillate," *Ind. Eng. Chem. Res.*, vol. 29, no. 4, p. 505, 1990.

[16] T. S. Nguyen, M. Tayakout-Fayolle, M. Ropars, and C. Geantet, "Hydroconversion of an atmospheric residue with a dispersed catalyst in a batch reactor: Kinetic modeling including vapor–liquid equilibrium," *Chem. Eng. Sci.*, vol. 94, pp. 214–223, May 2013.

[17] S. Sanchez, M. A. Rodriguez, and J. Ancheyta, "Kinetic mode for moderate hydrocracking of heavyoils," *Ind. Eng. Chem. Res.*, vol. 44, pp. 9409–9413, 2005.

[18] M. J. Angeles, C. Leyva, J. Ancheyta, and S. Ramírez, "A review of experimental procedures for heavy oil hydrocracking with dispersed catalyst," *Catal. Today*, vol. 220–222, pp. 274–294, Mar. 2014.

[19] D. Levin and J. Y. Ying, "The Structure and Defect Chemistry of Non-Stoichiometric Nickel Molybdates," vol. 3, pp. 25–36, 1999.

[20] A. A. Avidan and R. Shinnar, "Development of catalytic cracking technology. A lesson in chemical reactor design," *Ind. Eng. Chem. Res.*, vol. 29, no. 6, pp. 931–942, 1990.

[21] I. Pitault, D. Nevicato, M. Forissier, and J.-R. Bernard, "Kinetic model based on a molecular description for catalytic cracking of vacuum gas oil," *Chem. Eng. Sci.*, vol. 49, no. 24, pp. 4249–4262, 1994.

[22] M. Rashidzadeh, A. Ahmad, and S. Sadighi, "Studying of Catalyst Deactivation in a Commercial Hydrocracking Process (ISOMAX)," *J. Pet. Sci. Technol.*, vol. 1, no. 1, pp. 46–54, 2011.

[23] L.-S. Lee, Y.-W. Chen, T.-N. Huang, and W.-Y. Pan, "Four-lump kinetic model for fluid catalytic cracking process," *Can. J. Chem. Eng.*, vol. 67, no. 4, pp. 615–619, 1989.

[24] G. M. Bollas, A. A. Lappas, D. K. Iatridis, and I. A. Vasalos, "Five-lump kinetic model with selective catalyst deactivation for the prediction of the product selectivity in the fluid catalytic cracking process," *Catal. Today*, vol. 127, no. 1–4, pp. 31–43, 2007.

[25] M. Al-Sabawi, J. A. Atias, and H. De Lasa, "Kinetic modeling of catalytic cracking of gas oil feedstocks: Reaction and diffusion phenomena," *Ind. Eng. Chem. Res.*, vol. 45, pp. 1583–1593, 2006.

[26] M. Egorova and R. Prins, "The role of Ni and Co promoters in the simultaneous

HDS of dibenzothiophene and HDN of amines over Mo/??-Al2O3 catalysts," *J. Catal.*, vol. 241, pp. 162–172, 2006.

[27] S. H. Moon, "Effect of acidic and basic species on the hydrodesulfurization of methyl-substituted dibenzothiophenes," *Catal. Surv. from Asia*, vol. 7, no. 1, pp. 11–20, 2003.

VITAE

Name	Ahmad Hassan Ali Al-Rashidy
Nationality	Egyptain
Date of Birth	April 19, 1989
Email	ahmad.lrashidy@gmail.com
Address	18 Ebrahim Al-Attar St. Zezenya Alexandria, Egypt
Academic Background	B.Sc. in Gas and Petrochemical Engineering (1st Class) Alexandria University of Engineering Alexandria, Egypt M.Sc. in Chemical Engineering (Distinction) King Fahd University of Petroleum and Minerals Dhahran, Saudi Arabia December, 2015
Journal Publications	Al-Rashidy A.H., Ali S.A, Ahmed S., Razzak S.A., Hossain M.M., Phenomenological Kinetics Modeling of Simultaneous HDS of Dibenzothiophene and Substituted Dibenzothiophene over CoMoP/Al2O3 Catalysts, *Chemical Engineering Research and Design*
Conference papers	Al-Rashidy A.H., Razzak S.A., Hossain M.M., Hydrocracking of Heavy Oil in Supercritical Conditions using Fe-based Catalysts, 65th Canadian Chemical Engineering Conference, October 4-7, 20145 Calgary, Ontario, Canada.